JCI The Journal of Clinical Investigation

CD69 expression on regulatory T cells protects from immune damage after myocardial infarction

Rafael Blanco-Domínguez, … , José Martínez-González, Pilar Martín

J Clin Invest. 2022. https://doi.org/10.1172/JCI152418.

Research In-Press Preview **Cardiology** **Immunology**

Graphical abstract

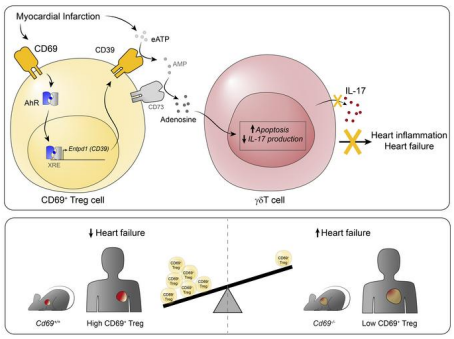

CD69 expression on regulatory T cells protects from immune damage after myocardial infarction

One sentence summary: CD69^{+} Treg cells protect from myocardial damage

Rafael Blanco-Domínguez [1], Hortensia de la Fuente [2,3], Cristina Rodríguez [3,4,5], Laura Martín-Aguado [1], Raquel Sánchez-Díaz [1, 3], Rosa Jiménez-Alejandre [1], Iker Rodríguez-Arabaolaza [1], Andrea Curtabbi[1], Marcos M. García-Guimaraes [6], Alberto Vera [6], Fernando Rivero [6], Javier Cuesta [6], Luis J. Jiménez-Borreguero [3,6], Alberto Cecconi [6], Albert Duran [7], Manel Taurón [7], Judith Alonso [3, 5, 8], Héctor Bueno [1, 3, 9, 10], María Villalba-Orero [1, 11], Jose Antonio Enríquez [1, 12], Simon C Robson [13], Fernando Alfonso [3, 6], Francisco Sánchez-Madrid [1, 2, 3], José Martínez-González [3, 5, 8] and Pilar Martín [1, 3,*]

[1] *Vascular Pathophysiology Area, Centro Nacional de Investigaciones Cardiovasculares (CNIC),* Madrid, Spain.

[2] *Department of Immunology, IIS Princesa, Hospital Universitario de la Princesa, Universidad Autónoma de Madrid,* Madrid, Spain.

[3] *CIBER de Enfermedades Cardiovasculares (CIBERCV),* Madrid, Spain.

[4] *Institut de Recerca del Hospital de la Santa Creu i Sant Pau,* Barcelona, Spain.

[5] *Instituto de Investigación Biomédica Sant Pau (IIB-Sant Pau),* Barcelona, Spain

[6] *Department of Cardiology, IIS Princesa, Hospital Universitario de la Princesa, Universidad Autónoma de Madrid,* Madrid, Spain.

[7] *Hospital de la Santa Creu i Sant Pau,* Barcelona, Spain.

[8] *Instituto de Investigaciones Biomédicas de Barcelona -Consejo Superior de Investigaciones Científicas (IIBB-CSIC),* Barcelona, Spain.

[9] *Cardiology Department, Hospital Universitario 12 de Octubre and Instituto de Investigación Sanitaria Hospital 12 de Octubre (imas12),* Madrid, Spain.

[10] *Facultad de Medicina, Universidad Complutense de Madrid, Madrid, Spain.*

[11]*Departamento de Medicina y Cirugía Animal, Facultad de Veterinaria, Universidad Complutense de Madrid;* Madrid, Spain.

[12] *CIBER de Fragilidad y Envejecimiento Saludable (CIBERFES),* Madrid, Spain.

[13] *Department of Medicine, Harvard Medical School, Transplantation Research Center, Beth Israel Deaconess Medical Center, Boston, MA, USA.*

* Address for Correspondence:

Pilar Martín, PhD

Vascular Pathophysiology Area, Centro Nacional de Investigaciones Cardiovasculares (CNIC).

Calle Melchor Fernández Almagro, 3. 28029 Madrid, Spain.

Tel: +34 914531200

e-mail: pmartinf@cnic.es.

The authors have declared that no conflict of interest exists.

Abstract

Increasing evidences advocate for an important function of T cells in controlling immune homeostasis and pathogenesis after myocardial infarction (MI), although the underlying molecular mechanisms remain elusive. In this study, a broad analysis of immune markers in 283 patients revealed a significant CD69 overexpression on Treg cells after MI. Our results in mice showed that CD69 expression on Treg cells increased survival after left-anterior-descending coronary artery (LAD)-ligation. *Cd69*$^{-/-}$ mice developed strong IL-17^{+} γδT cell responses after ischemia that increased myocardial inflammation and, consequently, worsened cardiac function. CD69^{+} Treg cells, by induction of AhR-dependent CD39 ectonucleotidase activity, induced apoptosis and decreased IL-17A production in γδT cells. Adoptive transfer of CD69^{+} Treg cells to *Cd69*$^{-/-}$ mice after LAD-ligation reduced IL-17^{+} γδT cell recruitment, thus increasing survival. Consistently, clinical data from two independent cohorts of patients indicated that increased CD69 expression in peripheral blood cells after acute MI was associated with a lower risk of re-hospitalization for heart failure (HF) after 2.5 years of follow-up. This result remained significant after adjustment for age, sex and traditional cardiac damage biomarkers. Our data highlight CD69 expression on Treg cells as a potential prognostic factor and a therapeutic option to prevent HF after MI.

Introduction

Myocardial infarction (MI) is an acute ischemic myocardial insult that clinically represents the global leading cause of mortality. Inflammation plays an essential role in the pathophysiology of atherosclerosis, plaque formation and plaque rupture, the main trigger of MI, but also in the process of myocardial healing and repair after ischemia-induced damage (1). The role of innate immunity and myeloid cells after MI has been widely studied (1, 2) but that of the adaptive immunity remains scarcely explored. Recent studies have shown that $CD4^+$ T cells are important contributors to inflammatory mechanisms and, more specifically, to myocardial damage repair mechanisms after ischemia-reperfusion processes (3, 4). Indeed, $CD4^+CD25^+Foxp3^+$ regulatory T (Treg) cells have emerged as important players in protection against cardiac damage after experimental MI (5). MI induces a cardioprotective T-cell response (6) and a rapid recruitment of Treg cells to the injured myocardium, mediated by the CXCL12/CXCR4 axis (7) and Galectin-1 (8). In parallel, Treg cells become activated 7 days after MI in the heart-draining lymph nodes (9) with increased percentages and absolute numbers, protecting from uncontrolled inflammation and cardiac deterioration. Indeed, Treg cell depletion aggravates cardiac inflammation and worsens prognosis early after experimental MI (9, 10). However, the specific molecular mechanisms that operate in these processes remain elusive.

Different studies in patients indicate that the proportions of Treg cells change in peripheral blood after MI (11-13). In addition, some evidence indicates that Treg cells accumulate in coronary thrombi (14) and in the heart (6) of MI patients, reinforcing the notion that Treg cells play a major role at the site of injury. Studies in larger cohorts of patients and exploration of different Treg cell regulatory molecules may further clarify the function of these cells after MI.

Cluster of differentiation (CD)69 is a C-type lectin whose gene is encoded within the natural killer cell gene complex on chromosome 6 and 12 in mouse and human, respectively. CD69 promotes immune homeostasis by regulating the differentiation and function of Treg cells (15, 16). Based on CD69 expression, Treg cells are classified into two subtypes: $CD69^+$ and $CD69^-$ Treg cells. $CD69^+$ Treg cells express higher levels of suppression markers such as CTLA-4, ICOS, CD38 and GITR than $CD69^-$ or *Cd69*$^{-/-}$ Treg cells, resulting in enhanced effector T-cell suppression and tolerance (15). *Cd69*$^{-/-}$ mice exhibit uncontrolled Th17 cell ($CD3^+CD4^+IL\text{-}17^+$) responses and aggravation of multiple autoimmune and inflammatory disease models (17), including those of the cardiovascular system such as atherosclerosis (18), myocarditis and inflammatory dilated cardiomyopathy (19). Other studies highlight that IL-17 exacerbates fibrosis and cardiac remodeling after MI (20, 21), although the involvement of Th17 cells after cardiac injury remains controversial. $CD3^+TCR\gamma\delta^+$ ($\gamma\delta$T) cells, which rapidly accumulate in the infarcted myocardium (22), are the main source of IL-17 during the first week after MI and appear to be associated with the morbidity of MI in mice (23) and patients (24).

There is evidence linking CD69 expression on T cells to MI. Interestingly, natural ligands of CD69, such as Gal-1(25) or S100A8/A9 (26), are upregulated after MI and contribute to immune cell recruitment (8, 27). Furthermore, CD69 is overexpressed on infiltrating T cells in the atherosclerotic plaques (28) and circulating $CD4^+$ T lymphocytes of MI patients, where it has been associated with increased apoptosis driven by lymphocyte activation (29). Therefore, we postulated that CD69 expression on lymphocytes might be a player in the post-MI progression towards chronic scenarios.

Many classical clinical and anatomic factors have been involved in the prognosis of MI patients. In these patients, early reperfusion followed by guideline-based medical therapy represents the

cornerstone of clinical management. However, predictive models, capable of identifying MI patients at higher risk for adverse long-term clinical outcomes, remain limited (30). Consequently, the use of additional markers capable of improving risk stratification after MI to select patients most likely to benefit from closer clinical follow-up, or more aggressive therapeutic strategies, would be desirable.

This study reveal that increased $CD69^+$ Treg cells are a common feature of mouse and patient peripheral blood shortly after MI. In addition, we describe a novel mechanism by which $CD69^+$ Treg cells control inflammation and cardiac damage after coronary artery ligation through inhibition of pathogenic $IL\text{-}17^+$ γδT cells. Finally, in the clinical setting, we found that Treg cells with low CD69 expression after acute MI are associated with an increased risk of re-hospitalization for heart failure at mid-term follow-up. Therefore, our data suggest that CD69 expression on Treg cells could be a promising candidate to improve the management of MI patients.

Results

Enhanced peripheral CD69$^+$ Treg cell response in patients with acute MI

The blood immune phenotype was determined in a cohort of 283 participants with acute myocardial infarction (MI) and 80 healthy volunteers (**Figure 1**). Demographic and clinical data are summarized in **Supplemental Table 1**. More than 90% of patients presented at least one risk factor, most frequently dyslipidemia, arterial hypertension and history of smoking. **Supplemental Table 1** also summarizes the results of biomarkers, electrocardiograph (ECG), coronary angiography (number of diseased vessels) and echocardiography (left ventricular segmental wall motion abnormalities and ejection fraction). Most patients presented as ST-segment elevation MI and the culprit lesion was more often located in the left-anterior descending (LAD) coronary artery or the right coronary artery, with 38.5% of patients presenting multivessel coronary artery disease. Left ventricular systolic function was generally preserved and only 1/3 of patients had a reduced left ventricular ejection fraction.

We performed an extensive analysis of lymphoid and myeloid cell populations by FACS in peripheral blood in the first 24 hours after the ischemic event (**Supplemental Figure 1A**). Elevation of serum cardiac damage markers, such as troponin T (TnT) and creatine kinase (CK), after MI are correlated with CD69 expression on circulating CD4$^+$ T cells and CD4$^+$CD25$^+$Foxp3$^+$ Treg cells as well as with the ratios of effector T cells versus CD69$^+$ Treg cells, suggesting that CD69 expression is induced upon myocardial damage (**Supplemental Table 2 and Supplemental Figure 1A**). Indeed, the analysis of CD4$^+$ T cells by flow cytometry revealed that a subset of CD69$^+$CD25$^+$Foxp3$^+$ Treg cells appear after MI (**Figure 1A**). CD4$^+$ T and Treg cell populations are decreased and augmented, respectively, in MI patients compared with healthy controls (**Figure 1B and Supplemental Figure 1B**). CD69 is virtually absent in

circulating blood lymphocytes due to the high concentration of sphingosine-1-phosphate (S1P) which maintains $S1P_1$ receptor levels high (31), suppressing CD69 expression (32). Therefore, we analyzed CD69 expression in circulating $CD4^+$ T cells in the blood after overnight bystander activation with anti-CD3 antibody. The percentage of $CD69^+$ Treg cells increases in the circulation in MI patients (**Figure 1C and Supplemental Figure 1C**), determined by an overall increase in CD69 expression on Treg cells after infarction in most patients (**Figure 1D**). However, we found two groups of patients according to CD69 expression levels on Treg cells, so we subdivided the population as patients with high CD69 expression (65% of patients) or low CD69 expression (35% of patients) for further analyses in this study (**Figure 1D**). Patients with high CD69 expression present lower percentages of $CD4^+$ T and IL-22^+CD4^+ T cells but higher percentages of Treg cells. In addition, high CD69 patients present more naïve and less memory Treg cells, according to the expression of $CD45RA^+$ and $CD45RO^+$, respectively (**Figure 1E and Supplemental Figure 1D**). Unsupervised hierarchical clustering of patients based on myeloid and lymphoid cell types analyzed by FACS (**Supplemental Figure 1A**) evidences that high and low CD69 patients present different immune phenotypes as they cluster in distinct groups (**Figure 1F**).

CD69 expression improves survival and recovery after LAD-ligation in mice

To evaluate the role of CD69 expression in recovery after MI, we analyzed the survival after ligation of the LAD coronary artery in mice. Survival was significantly reduced in *Cd69*$^{-/-}$ mice compared with their wild-type littermates (**Figure 2A**). *Cd69*-deficient mice recovered worse after infarction, as they were unable to reach baseline weight one week after LAD-ligation (**Figure 2B**). In addition, *Cd69*$^{-/-}$ mice showed elevated myocardial damage **(Figure 2C)** and

increased heart-weight to body-weight and heart-weight to tibia-length ratios two days after LAD-ligation, indicating that *Cd69*$^{-/-}$ hearts may be swollen perhaps as a consequence of greater inflammation **(Figure 2D)**. The assessment of infarct size and ischemic area at risk by the double staining with triphenyltetrazolium chloride (TTC) and Evan´s blue is a widely-used method for the quantification of myocardial damage after infarction (33). Infarct size of *Cd69*$^{+/+}$ mice ranges from 40 to 80 %, in agreement with previous reports in this model (34-36). The absence of CD69 leads to a significantly increased infarct size two days after infarction, supporting a higher tissue damage in these mice (**Figure 2E and 2F**). Two days after MI, mice wild-type and CD69-deficient mice showed several cardiac rhythm abnormalities, including ventricular premature depolarizations, first degree atrioventricular blocks and ST-segment elevation. However, under cardiac stress conditions induced by isoproterenol injection, *Cd69*$^{-/-}$ mice enhanced these cited cardiac arrhythmias than their wild-type littermates and eventually bradyarrhythmias led to complete heart block, ventricular scape rhythms and death (**Supplemental Figure 2**). Evaluation of cardiac function by echocardiography indicates that the ventricular wall motion score index increases in *Cd69*$^{-/-}$ mice as the disease progresses, reaching significance *versus* wild-type mice one month after infarction, supporting a worse prognosis in *Cd69*$^{-/-}$ mice after LAD-ligation (**Figure 2G**).

Since most patients with MI are eventually reperfused during admission, we analyzed the consequences of CD69 depletion in a mouse model of MI induced by ischemia and reperfusion (I/R). Similar to the data obtained with the permanent LAD-ligation model, *Cd69*$^{-/-}$ mice present increased cardiac dysfunction and worse weight recovery after I/R, resulting also in a slightly decreased survival (**Supplemental Figure 3**).

IL-17$^+$ γδT cells are the main source of peripheral IL-17A shortly after myocardial infarction and are increased in *Cd69*$^{-/-}$ mice

It is well known that the number of CD4$^+$CD25$^+$Foxp3$^+$ Treg cells increases in the heart during the first day after infarction (37), indicating an antigen-independent migration of Treg cells into the injured myocardium. We observed a specific mobilization of CD69$^+$ Treg cells in wild-type mice after infarction, with a 2.5-fold increase in peripheral blood in the first 24 hours (**Figure 3A**), mimicking the peripheral response in MI patients (**Figure 1**). This mobilization is not observed in either wild-type CD69$^-$ or *Cd69*$^{-/-}$ Treg cells (**Figure 3A**). Since *Cd69*$^{-/-}$ mice have exacerbated Th17 responses in different inflammatory diseases (38), we analyzed the kinetics of IL-17A$^+$ cells in blood one week after infarction. *Cd69*$^{-/-}$ mice have a significantly increased IL-17 response during the first 2-7 days after LAD-ligation, which is not observed in *Cd69*$^{+/+}$ mice (**Figure 3B**). The majority of IL-17A producing cells in peripheral blood after infarction are CD3$^+$ T cells (**Figure 3C**), being γδT cells, but not Th17 cells, the main source of IL-17 in the blood after infarction (**Figure 3C**). *Cd69*$^{-/-}$ γδT cells express higher levels of IL-17A even in steady state and *Cd69*$^{-/-}$ mice amplify the IL-17$^+$ γδT cell response in peripheral blood shortly after MI (**Figures 3D and 3E**). As IL-17$^+$ γδT cells are well known as initiators of inflammation (39) and induce apoptosis of cardiac myocytes (40), we postulate that this population may contribute to the increased damage observed in *Cd69*$^{-/-}$ mice after LAD-ligation.

IL-17$^+$ γδT cells rapidly accumulate in the infarcted myocardium in *Cd69*$^{-/-}$ mice

Next, we analyzed the leukocyte populations infiltrating the myocardium to characterize inflammation in infarcted tissue from *Cd69*$^{-/-}$ mice. Quantification of the total number of leukocytes per mg of infarcted tissue shows that the hearts of *Cd69*$^{-/-}$ mice exhibit increased

inflammation at day 2 after MI compared with their *Cd69*$^{+/+}$ littermates (**Figure 4A**). Consistent with previous studies, we found that Treg cells are recruited to the heart after ischemia. However, we found an increased number of CD69^{+} Treg cells and higher CD69 expression on Treg cells in the myocardium of MI mice *versus* sham mice, indicating a selective migration of these cells to the myocardium after LAD-ligation (**Figure 4B)**. The analysis of CD69 expression in different cardiac populations revealed that CD45^{-}CD31^{+} endothelial cells, CD45^{+}CD11b^{+} myeloid cells and CD45^{+}CD11b^{-}CD4^{+}Foxp3^{-} T effector cells do not upregulate CD69 after MI at the same extent than Treg cells (**Supplemental Figure 4A and 4B**). These data support a dominant role of CD69 in the Treg cell compartment after MI. In the infarcted myocardium, γδT cells peak one week after ischemia and are the main producers of IL-17 (23). Indeed, we confirmed that the majority of IL-17A producing cells are TCRγδ^{+} cells (about 75%) in both *Cd69*$^{+/+}$ and *Cd69*$^{-/-}$ mice, although γδT cells and IL-17^{+} γδT cells infiltration in the myocardium is significantly increased in *Cd69*$^{-/-}$ mice as early as two days after MI (**Figure 4C**). Neither *Cd69*$^{+/+}$ nor *Cd69*$^{-/-}$ mice show a significant recruitment of Th17 cells at this early time point (**Supplemental Figure 4C).** Furthermore, although no differences in the number of CD11b^{+} myeloid cells or CD11b^{+}Gr1^{hi} granulocytes are observed between genotypes, *Cd69*$^{-/-}$ mice show a higher number of inflammatory Ly6C^{hi} cells accumulated in the infarcted myocardium (**Figure 4D and Supplemental Figure 4D**), indicating a more pro-inflammatory phenotype (41). In parallel, the pathogenic IL-17^{+} γδT cell population is significantly increased in the mediastinal lymph nodes draining the heart after infarction in *Cd69*$^{-/-}$ mice (**Supplemental Figure 4E**).

CD69^{+} Treg cells induce apoptosis and reduce IL-17A production in γδT cells in a CD39-dependent manner in mice

Previous studies provide evidence for antigen-independent inhibition of γδT cells by Treg cells (42, 43), although the mechanisms remain poorly understood. Our data suggest that CD69 expression on Treg cells may be involved in limiting γδT cells activity. To test this hypothesis, we co-cultured sorted *Cd69*$^{+/+}$ or *Cd69*$^{-/-}$ Treg cells with *Cd69*$^{+/+}$ γδT cells from peripheral lymph nodes (**Supplemental Figure 5A and 5B**). Our data indicate that CD69^{+} Treg cells induce apoptosis in γδT cells more efficiently than *Cd69*$^{-/-}$ Treg cells (**Figure 5A**). Both *Cd69*$^{+/+}$ and *Cd69*$^{-/-}$ Treg cells successfully decrease IL-17A production in a dose-dependent manner. However, at lower numbers of Treg cells, *Cd69*$^{+/+}$ Treg cells show more significant reduction of IL-17A production (**Figure 5B**).

CD39 is a membrane ectonucleotidase expressed in most Treg cells that, together with CD73, transforms extracellular ATP to adenosine (44, 45). It has been shown that CD39 on Treg cells can mediate inhibition of innate (46) and non-immune cells (47) by immunosuppression-independent mechanisms upon tissue injury. We have evaluated whether the observed inhibition of γδT cells by CD69^{+} Treg cells after infarction is mediated by CD39. Our data show that CD69^{+} Treg cells express higher levels of membrane CD39 than CD69^{-} and *Cd69*$^{-/-}$ Treg cells in peripheral blood, mediastinal lymph nodes and cardiac infiltrate two days after MI (**Figure 5C**). Sorted *Cd69*$^{+/+}$ Treg show also an increased extracellular ATP consumption compared to *Cd69*$^{-/-}$ Treg cells. The addition of ARL 67156, a chemical inhibitor of CD39, reduced ATP consumption of *Cd69*$^{+/+}$ Treg and abolished differences between genotypes (**Figure 5D**). These results support that CD39 activity is impaired in CD69-deficient Treg cells. Regarding the observed reduction of IL-17A production in γδT cells by CD69^{+} Treg cells (**Figure 5B**), it is reverted in the presence of the inhibition of ARL 67156, while no effect of is observed on *Cd69*$^{-/-}$

Treg (**Figure 5E**). A direct effect of ARL 67156 on γδT cells was ruled out since no γδT cell inhibition is observed when adding ARL 67156 in the absence of Treg cells.

Aryl Hydrocarbon Receptor (AhR) is one of the main factors that mediates CD39 expression. Ligand-dependent activation of AhR induces *Entpd1* (CD39 encoding gene) expression through direct binding to XRE regions of the *Entpd1* promoter (48). Our data also validate that *Entpd1* mRNA levels, as well as CD39 activity, were reduced in *Ahr*$^{-/-}$ Treg cells, supporting that AhR is a dominant transcription factor for *Entpd1* expression in this cell type (**Supplemental Figure 5C and 5D**). We have previously described that CD69 allows the uptake of AhR ligands such as L-Tryptophan in T cells by association with the aromatic-amino-acid-transporter complex on the membrane, allowing activation of AhR (49). We observed that Treg cells lacking CD69 exhibit decreased expression of AhR transcriptional targets, including *Cyp1b1* and, importantly, *Entpd1* (**Figure 5F**). Additionally, AhR-deficient CD69^{+} Treg cells exhibits decreased CD39 expression compared to wildtype Treg cells (**Supplemental Figure 5E**), supporting that AhR-signaling mediates CD39 expression in CD69^{+} Treg cells. Together, these data suggest that CD69 expression on Treg cells allows AhR-mediated expression of CD39, increasing ATP conversion to adenosine that triggers inhibition of pathogenic IL-17^{+} γδT cells and controls inflammation after MI.

Adoptive transfer of CD69-sufficient Treg cells into *Cd69*$^{-/-}$ mice restores survival, inflammation and cardiac damage after MI

Next, we performed adoptive transfer experiments to assess the specific role of CD69 on Treg cells in the control of inflammation and recovery after infarction. In vitro differentiated Treg

cells (iTreg) from naïve *Cd69*$^{+/+}$ and *Cd69*$^{-/-}$ CD4^{+} T cells (**Supplemental Figure 6A**) were injected intravenously into *Cd69*$^{-/-}$ mice 4-5h after LAD-ligation and mice were monitored for one week (**Figure 6A**). Therapy with *Cd69*$^{+/+}$ iTreg cells improved survival of *Cd69*$^{-/-}$ mice after infarction (**Figure 6B**). Furthermore, the heart-to-body weight ratio was preserved in the *Cd69*$^{-/-}$ mice transferred with *Cd69*$^{+/+}$ iTreg cells, as was the total number of leukocytes infiltrating the myocardium (**Figure 6C**). CD69 expression drives CD39 expression in myocardial Treg and T effector cells, although CD69^{+} Treg cells exhibit the highest CD39 levels (**Supplemental Figure 6B**). Interestingly, infiltrating IL-17A^{+} γδT cells are reduced in the myocardium after transfer of *Cd69*$^{+/+}$ iTreg but not *Cd69*$^{-/-}$ iTreg cell, supporting a CD69-mediated inhibition of this population by Treg cells (**Figure 6D**). In parallel, myeloid cells, including pro-inflammatory Ly6C^{hi} monocytes, are also reduced (**Supplemental Figure 6D**). All these data suggest that CD69-expressing Treg cell transfer reverts the immune-mediated cardiac damage after MI in *Cd69*$^{-/-}$ mice. Interestingly, when ARL 67156 is administered in vivo to inhibit CD39, *Cd69*$^{+/+}$ iTreg cells lose their ability to restore survival, myocardial inflammation and IL-17A^{+} γδT cell accumulation in the heart (**Figure 6E-G)**), suggesting that the therapeutic effects of *Cd69*$^{+/+}$ iTreg cell transfer is CD39-dependent. Transfer of *Cd69*$^{+/+}$ iTreg to wild type infarcted mice (**Supplemental Figure 7A**) also improve myocardial inflammation and survival better than the transfer of *Cd69*$^{-/-}$ iTreg cells, although without reaching significance probably due to the presence of endogenous CD69^{+} Treg cells (**Supplemental Figure 7B and 7C**). Likely for the same reason, no differences in myocardial γδT cells are found in transferred wild type mice (**Supplemental Figure 7D**).

Early expression of CD69 on Treg cells is associated with a lower risk of heart failure development in MI patients

The prognostic value of CD69 expression after MI was tested in those patients who completed follow-up at the time of the manuscript writing. The mean clinical follow-up time of our primary study population was 2.5 years (**Supplemental Table 3**). CD69 expression on Treg cells, measured at the time of hospital admission during index MI, was lower in patients who were subsequently re-hospitalized for heart failure (HF) (**Figure 7A**). Interestingly, left-ventricular ejection fraction, but not CK or Troponin T levels, also decreased during MI in patients who subsequently developed HF (**Supplemental Figure 8A**). After stratifying patients according to high or low CD69 expression, as in **Figure 1D**, we observed that most patients who developed HF within the first 2.5 years after MI belonged to the group expressing low membrane CD69 levels on Treg cells (**Figure 7B**). Determination of *CD69* mRNA expression by qPCR in total PBLs also revealed association with disease outcome, as most of those patients expressing low *CD69* mRNA levels developed HF (**Figure 7C**). *CD69* mRNA levels correlates with surface CD69 levels, associating CD69 protein and transcript expression (**Supplemental Figure 8B**), and with *FOXP3* mRNA levels, highlighting a predominant CD69 expression by Treg cells (**Figure 7D**). The equivalence in measuring CD69 by qPCR or by FACS supports the use of either method for the prediction of HF development. Importantly, the percentage of $CD69^+$ Treg cells remains as an independent predictor of the development of HF after adjusting for the levels of cardiac damage, age and sex (**Table 1**).

In parallel, we prospectively analyzed the association of early CD69 expression (during the first 24h from hospitalization due to MI) with clinical outcome after MI in an additional independent validation cohort of 84 patients with similar follow-up times (**Supplemental Tables 4 and 5**).

Quantification of *CD69* mRNA levels in frozen PBLs confirmed that patients who developed HF expressed lower *CD69* levels at acute MI. (**Figures 7E and 7F**). Although CD69 expression on the surface of Treg cells was not available in this cohort, *CD69* mRNA expression correlated significantly with *Foxp3* expression, establishing an association between CD69 expression and the Treg subset, as in the main patient cohort (**Figure 7G**). Thus, these data support that CD69 expression during acute MI is associated with a lower risk of developing HF after MI.

Discussion

This study identifies CD69 as a key Treg cell receptor for controlling immune-mediated myocardial damage early after MI. We observed a specific deployment of $CD69^+$ Treg cells in the peripheral blood of MI patients and LAD-ligation mice. Moreover, CD69-deficient mice and patients with low CD69 levels shortly after acute MI have a worse prognosis after the ischemic event.

The general idea is that Treg cells are recruited to the myocardium during the first few days after MI to control excessive inflammation and prevent cardiac deterioration (7, 9, 10, 37, 50). We have recently shown that CD69 expression on lymphocytes prevents atherosclerosis progression in mice, and that low CD69 levels in peripheral blood leukocytes predict subclinical atherosclerosis in asymptomatic individuals after adjustment for traditional cardiovascular risk factors (18). Here we describe for the first time that CD69 expression is pivotal for the anti-inflammatory properties of Treg cells after ischemic myocardial damage. CD69 expression in T cells is an inflammatory brake that promotes Treg cell differentiation and suppressor function and prevents pro-inflammatory T cell responses in multiple disease scenarios (38). In this study, we describe a novel mechanism by which CD69 expression on Treg cells promotes antigen-independent inhibition of pro-inflammatory γδT cells after MI. CD69 induces AhR-dependent CD39 expression and extracellular ATP conversion to adenosine, inhibiting effector cytokine production and inducing apoptosis in γδT cells infiltrating the ischemic myocardium.

Mice lacking CD69 show increased myocardial inflammation and dysfunction, leading to a rapid decrease in survival during the first week after infarction. Therapy with $CD69^+$ Treg cells in the first hours after LAD-ligation reduces myocardial inflammation and improves survival of *Cd69*$^{-/-}$

mice, indicating that CD69 expression specifically on the Treg subset is sufficient to alleviate the recovery after MI.

Acute MI is the leading cause of mortality worldwide, with HF secondary to MI as one of the most important complications (51). In a follow-up of two independent clinical cohorts, we found that patients who were re-hospitalized due to HF had lower CD69 expression within the first hours after acute MI. Even after adjusting by age, sex and the level of cardiac damage, CD69 expression on Treg cells remains as an independent predictor of HF development after MI. Thus, in agreement with the phenotype observed in mice, CD69 expression during MI is associated with a better clinical outcome in these patients. Although these results have been validated in two independent cohorts with multivariate adjustment, the number of patients who developed HF is small. Therefore, our findings should be reproduced in larger cohorts, ideally including a longer time interval after MI.

In order to shed light on the regulatory mechanism of CD69 after MI, we explored the inflammatory signature in a mouse model of LAD-ligation. We found that the absence of CD69 results in a rapid and detrimental excess of inflammatory infiltrating leukocytes in mice as early as two days after LAD-ligation. Increased numbers of IL-17^{+} γδT cells characterize the cellular heart infiltrate of *Cd69*$^{-/-}$ mice, being the main source of IL-17A early after MI. The increased recruitment of IL-17^{+} γδT cells could explain the worse prognosis of *Cd69*$^{-/-}$ mice after MI, as γδT cells induce cardiomyocyte apoptosis (40) and their production of IL-17 promotes fibrosis, sustains neutrophil/monocyte infiltration and polarizes macrophages towards a pro-inflammatory phenotype (23). We observed that peripheral *Cd69*$^{-/-}$ γδT cells express significantly higher levels of IL-17A under basal conditions, suggesting that CD69 may be also playing a role in the generation of this T cell subset. We found that CD69^{+} Treg cells are significantly recruited to the

infarcted myocardium, but *Cd69*$^{-/-}$ mice show an even higher total number of Treg cells in the myocardium at this time point, probably due to a parallel compensatory anti-inflammatory response to balance the tissue damage.

Interestingly, the accumulation of IL-17^{+} γδT cells in the myocardium is impaired when *Cd69*$^{+/+}$ but not *Cd69*$^{-/-}$ Treg cells are transferred, suggesting that Treg cells inhibit IL-17^{+} γδT cells by a mechanism involving CD69. It is well established that Treg cells suppress effector CD4^{+} T cells and CD8^{+} T cells (52, 53). However, these cell populations play a minor a role after MI. It has been described that Treg cells can reduce the proliferation of human phosphoantigen-expanded γδT cells (43) and the proliferation and cytokine production of murine intestinal γδT cells (42) in an antigen-independent manner, suggesting that Treg cells are also capable of inhibiting this T cell subset. Our data show that mouse γδT cells undergo apoptosis and decrease IL-17A production in vitro in the presence of Treg cells, supporting the inhibitory effect of Treg cells on γδT cells. This effect is dose-dependent and is mediated by CD69, as *Cd69*$^{-/-}$ Treg cells show a lower inhibitory capacity. These results may explain the decrease in the number of IL-17A^{+} γδT cells in the infarcted myocardium after the adoptive transfer of *Cd69*$^{+/+}$ Treg cells.

In order to further explore in the molecular basis of this rapid inhibition of γδT cells, we examined the CD39-mediated antigen-independent mechanisms of Treg suppression. CD39 is an ectonucleotidase that hydrolyzes extracellular ATP, released from damaged tissue, to AMP, which is further degraded to adenosine by CD73. Uptake of adenosine by innate and T effector cells promotes apoptosis and cell inhibition (45, 46), but uptake by Treg cells induce anti-inflammatory properties (54). Treg cells from MI patients overexpress CD39 early after revascularization (10). Our work shows that CD69^{+} Treg cells infiltrating peripheral blood, draining lymph nodes and heart express higher levels of membrane CD39 compared with CD69^{-}

or *Cd69*$^{-/-}$ Treg cells two days after MI. Since CD69 facilitates the entrance of AhR ligands (49), the increased expression and activity of CD39 (transcriptional target of AhR) in CD69-sufficient Treg cells could be explained by the observed increased activation of the AhR pathway. In agreement, different studies described that CD39 confers protection after infarction, showing that CD39 overexpression ameliorates the progression after MI (55-57) or that *Cd39*$^{-/-}$ mice developed exacerbated cardiac damage (58). Moreover, adoptive transfer of *Cd39*$^{-/-}$ iTreg cells fails to prevent inflammation and achieve cardiac protection after MI (10). Thus, Treg cells deficient for either CD69 or CD39 present similar dysfunctional properties early after MI. Consistently, we report that chemical inhibition of CD39 in vitro and in vivo results in impaired suppression of γδT cells by CD69-sufficient Treg cells, suggesting that CD69^{+} Treg cells exert their inhibition of γδT in a CD39-dependent manner. All these evidences suggest a novel molecular mechanism of Treg protection against inflammatory-mediated cardiac impairment, although a further exploration in a clinical setting is needed.

In conclusion, we have identified CD69 as a new crucial orchestrator of the cardioprotective function of Treg cells after MI. Although further studies are needed to prospectively confirm the diagnostic and therapeutic value of circulating CD69^{+} Treg cells, this target opens new specific cellular avenues for precision medicine to improve the management of MI patients.

Methods

Study design

The overall objective of our study was to investigate the relevance of CD69-expressing Treg cells in the progression after MI. For this purpose, we analyzed the expression of CD69 on Treg cells in peripheral blood of MI patients. In addition, in order to deepen in the mechanism of action of these cells, we performed permanent LAD-ligation to induce MI in *Cd69*$^{-/-}$ mice and their *Cd69*$^{+/+}$ littermates. Peripheral immune response and heart inflammation, necrosis and function were evaluated. We also transferred *Cd69*$^{-/-}$ infarcted mice with CD69-sufficient iTreg cells to narrow down the protective effect of CD69 to the Treg cell compartment. Further in vitro experiments adding Treg cells to γδT cell cultures were performed to prove a direct CD69-dependent inhibitory effect on γδT cells.

The genotyping of mice were recorded throughout the entire period of the study. Mice were randomly assigned to each experimental group, the only criteria used to stratify was the genotype. Infarct size quantification was performed in a blind manner. Fur survival plots, mice that died during the surgical procedure were excluded. We also excluded animals with undetectable/marginal infarct zone observed by echocardiography two days post-surgery, probably due to an unsuccessful LAD-ligation. For all the experiments, sample sizes were determined by our previous data with similar experiments and prior literature to ensure statistical relevance. Numbers of replicates and statistical tests are indicated in the figure legend. We used at least three biological replicates for every assay, and each experiment was performed at least three times when applicable.

All blood samples from patients with suspicion of meeting all the MI inclusion criteria were blindly processed upon hospital admission, during the period of the study. Only patients that

were confirmed as MI after extensive diagnosis and met the inclusion criteria were included in the analyses. Data from patients with uncertain diagnosis were excluded. Blood samples from patients processed more than 24h post-extraction were also excluded from the study, since degradation of blood components might have altered the sample. The number of human samples was determined according to an estimation of clinical relevance. The incidence of HF and death was assessed in the patients with MI in which FACS was measured and a follow-up was available at the time of manuscript production. A similar N of healthy volunteers with normal ECG and heart function measured by echocardiography were included in the study as comparators.

Human blood sample collection included in the study

Blood samples of MI patients were prospectively collected from the arterial sheath used for coronary angiography and percutaneous coronary interventions prior to the administration of heparin, between March 2017 and May 2019. All demographic, clinical, angiographic and procedural characteristics of these patients with MI were also prospectively collected. Revascularization and subsequent clinical management at the coronary care unit and at the cardiology ward was performed following the guideline recommendations for MI (30) (**Table S1 and S3**). All patients with MI were systematically followed in a dedicated outpatient clinic.
In parallel, we analyzed blood samples from 80 healthy donors without any cardiac disease, as assessed by normality of cardiac markers, electrocardiography and echocardiography.
The validation cohort consisted of a consecutive series of patients admitted to the Hospital de la Santa Creu i Sant Pau, Barcelona, Spain, for MI. Baseline clinical characteristics, clinical presentation and in-hospital evolution are summarized in **table S4.** All patients were followed and the predefined adverse clinical outcomes (HF and all-cause death) are summarized in **table**

S5. Blood samples were collected within the first 24 h from the admission and prior to heparin administration.

Mice

CD69-deficient mice were generated as described previously (15). Wild- type or CD69-deficient mice used for experiments were 8-12 weeks-old males in a C57Bl/6 background. Foxp3-RFP/IL17-eGFP reporter mice were kindly provided by Dr. R. A. Flavell (Yale University) and crossed with *Cd69*$^{+/+}$ or *Cd69*$^{+/+}$ mice. Different experimental groups were sex- and age-matched with the offspring of littermate mice. Animals were housed and used under specific-pathogen-free (SPF) conditions at the Centro Nacional de Investigaciones Cardiovasculares (CNIC) animal facility.

Mouse model of myocardial infarction

For MI induction, a permanent ligation of the LAD coronary artery was performed. Briefly, mice were anesthetized with sevoflurane (4%), and intubated using a 24-gauge catheter with a blunt end. Mice were artificially ventilated with a mixture of O_2 and air (1:1, vol:vol) using a rodent ventilator (minivent 845, Harvard) with 160 strokes/min in a total volume of 250 μl. Mice were placed on a heating pad to maintain body temperature at 37 °C. A thoracotomy was performed through the fourth left intercostal space, the pericardium was opened and the heart was exposed. The proximal LAD coronary artery was localized and permanently ligated by passing a 7-0 silk suture around the artery. Sham operated mice were analyzed in parallel as controls of surgery.

Mouse infarct size quantification

Animals were anesthetized and 0.5 ml of 1% (weight/volume) Evan's Blue dye was infused intravenously through the cava vein 36 hours post surgery. Rapidly we opened the thoracic cavity to perfuse hearts with PBS and wash out the excess of Evan's Blue. Heart was then harvested, rinsed and atria were removed. The hearts were photographed before being cut into transverse slices (4-5 per ventricle). Then, slices were weighted. The palish negative area for Evan's Blue delineates the area at risk (AAR): myocardium lacking blood flow. In order to differentiate infarcted from viable tissue, the same slices were then incubated in triphenyltetrazolium chloride (TTC, 1% (weight/volume) in PBS) at 37 °C for 15 minutes. The sections were then re-photographed and weighed. After the incubation with TTC, Evan's Blue staining clears out and sections present two areas: one necrotic (palish negative for TTC staining: infarcted myocardium) and one alive (red positive for TTC staining). Regions negative for Evan's Blue staining (AAR) and for TTC (infarcted myocardium) were blindly quantified using ImageJ with FIJI image processing package (NIH). Percentages of AAR and Infarcted myocardium were weighted and corrected independently for each slice, and the total mg of AAR and TTC-negative region was calculated for each heart. The AAR were determined as the mg:mg ratio of AAR:Ventricle weight, and the Infarct Size were determined as infarcted myocardium:AAR.

Electrocardiography acquisition in mice

Two days after LAD-ligation, mice were anesthetized with 0.5–2% isoflurane in oxygen, administered via nose cone and adjusting the isoflurane delivery to maintain the heart rate around 500±50 bpm. Surface electrocardiograms were obtained by using unipolar and bipolar limb leads for 5 minutes in basal conditions (Biopac Systems, Inc.). Then, 1.5 mg/kg of isoproterenol

(Sigma-Aldrich) was injected intraperitoneally, and electrocardiograms were monitored over 15-25 more minutes. Electrocardiograms were blindly analyzed by an expert using Acqknowledge version 4.1.1 for MP36R (BIOPAC Systems, Inc.).

Echocardiography acquisition in mice

Transthoracic echocardiography was performed by a blinded expert operator using a high-frequency ultrasound system (Vevo 2100, Visualsonics Inc., Canada) with a 30-MHz linear probe. Two-dimensional (2D) and M-mode (MM) echography were performed at a frame rate over 230 frames/sec. Mice were lightly anesthetized with 0.5-2% isoflurane in oxygen, adjusting the isoflurane delivery to maintain the heart rate in 450±50 bpm. Mice were placed in supine position and maintained normothermia using a heating platform and warmed ultrasound gel. A base apex electrocardiogram (ECG) was continuously monitored. Longitudinal and short axis views of the left ventricle were acquired at the papillary muscles level for M-mode and also medium and apical levels for 2D. For the analysis of the wall motion score using echocardiography, regional left ventricular function was evaluated in the parasternal long-axis view. The left-ventricular wall was subdivided into six segments (basal,mid, and apical in the anterior and posterior walls). Each segment was scored by an independent blinded evaluator based on its motion and systolic thickening, according to the guidelines of the American Society of Echocardiography(59): (1) normal or hyperkinetic, (2) hypokinetic (reduced thickening), (3) akinetic (absent or negligible thickening, e.g., scar), and (4) dyskinetic (systolic thinning or stretching, e.g., aneurysm). The number of dysfunctional segments was quantified, and the total wall motion score index (WMSI) representing the sum of the score of the six individual segments in each heart was calculated.

Isolation of infiltrating cells from mouse heart

Hearts were perfused with 10 ml of PBS and removed from the chest cavity. The hearts were then minced and digested with collagenase IV (100 U/mL; Gibco) for 45 minutes at 37 °C under constant agitation. The resulting cell suspensions were filtered through 40-µm cell strainers (BD Falcon) and washed twice with phosphate-buffered saline (PBS), 0.5% bovine serum albumin (BSA), 1 µM EDTA. Erythrocytes were removed using hypotonic buffer. The number of leukocytes was assessed. Single cell suspensions were stained as follows and the different cell populations where analyzed by FACs.

FACS analysis

Peripheral Blood Leukocytes (PBLs) were isolated from mouse or human blood samples using Ficoll-Isopaque (density=1.121 g/ml) gradient centrifugation. Human/Mouse PBLs or single cell suspensions of mouse lymph nodes or heart infiltrating leukocytes were incubated in PBS +0.05% BSA +0.01% EDTA buffer with fluorochrome-conjugated antibodies. PBLs were stained in fresh for myeloid cell markers and cultured overnight for bystander activation in plates coated with 3 µg/ml purified anti-CD3 (for human cells: OKT3 clone, Biolegend; for mouse cells: 145-2C11 clone, BD PharMingen) in complete RPMI medium (20% FBS, Gibco) prior to T cell staining.

For human Foxp3 evaluation, nuclear staining was performed using the Foxp3 staining buffer set (Miltenyi Biotec) according to the provider's instructions.

For cytokine production assessment, cells were stimulated with 50 ng/ml phorbol myristate acetate (PMA, Sigma Aldrich), 1 µg/ml ionomycin (Sigma Aldrich) and 1 µg/ml GolgiPlug (BD

PharMingen) in complete culture medium for 4 additional hours. For cytokine-producing T helper cell evaluation, cells were fixed with PBS 2% paraformaldehyde for 10 minutes at room temperature and intracellularly stained with conjugated-antibodies in PBS +0.05% BSA +0.01% EDTA +0.5% saponin.

The following monoclonal antibodies were used for staining of different human markers in human samples: anti-CD14 (clone: M5E2, Biolegend), anti-CD16 (clone: DJ130, Dako), anti-CD25 (clone: 2A3, BD Biosciences), anti-CD4 (clone: SK3, BD Biosciences), anti-CD45RA (clone: H100, BD Biosciences), anti-CD45RO (clone: UCHL1, BD Biosciences), anti-CD66b (clone: G10F5, Biolegend), anti-CD69 (clone: FN50, BD Biosciences), anti-Foxp3 (clone: 3G3, Miltenyi Biotec), anti-HLA-DR (clone: G46-6,BD Biosciences), anti-IFNγ (clone: B27, BD Biosciences), anti-IL-17A (clone: SCPL1362, BD Biosciences) and anti-IL-22 (clone: 142928, R&D Systems). For mouse samples, the following antibodies were used: anti-CD11b (clone: M1/70, BD Biosciences), anti-CD3 (clone: 145-2C11, Biolegend), anti-CD4 (clone: RM4-5, BD Biosciences), anti-CD45.2 (clone: 104, Biolegend), anti-CD69 (clone: H1.2F3, BD Biosciences), anti-F4/80 (clone: BM8, Biolegend), anti-Gr1 (clone: RB6-8C5, BD Biosciences), anti-IL-17A (clone: TC11-18H10, BD Pharmingen), anti-Ly6C (clone: AL-21, BD Biosciences) and anti-TCRγδ (clone: GL3, Biolegend).

Cells were analyzed in a LSRFortessa or FACSymphony Flow Cytometer and the data were processed with FlowJo v10.0.4 (Tree Star).

Adoptive transfer of Treg cells

Naive $CD4^+$ T cells were purified from single-cell suspensions of the spleen and mesenteric lymph nodes of Foxp3-mRFP/IL17-eGFP/*cd69*$^{+/+}$ or Foxp3-mRFP/IL17-eGFP/*cd69*$^{-/-}$ reporter mice. Cell suspensions were incubated with biotinylated antibodies against CD44, CD8, major

histocompatibility complex (MHC) class II (I-Ab), CD19, B220, IgM, CD11b, CD11c, and DX5 and subsequently with Streptavidin Microbeads (MACS; Miltenyi Biotec). Naïve $CD4^+$ T cells were negatively selected in LD columns (MACS; Miltenyi Biotec) according to the manufacturer's instructions. The naïve status was confirmed by expression of CD4 and CD62L by flow cytometry (data not shown). Naïve $CD4^+$ T cells (10^6 cells/ml) were co-cultured for 72h with irradiated (30 Gy) antigen presenting cells in the presence of plate-bound anti-CD3 (2 µg/ml) and soluble anti-CD28 (2 µg/ml) plus recombinant TGF-β1 (10 ng/ml) and IL-2 (2 ng/ml) in RPMI medium (Gibco). After determining the purity of $CD4^+CD25^+Foxp3^+$ cells, 1.5 x 10^6 iTreg cells were intravenously injected to *Cd69*$^{-/-}$ mice 4-6 h after LAD ligation. In the indicated experimental groups, ARL 67158 (0.26 mg/kg mice, Tocris) was intraperitoneally administered in PBS at 4-6h, 48h and 96h after MI. Mice treated with PBS alone were used as controls. Mice were sacrificed 7 days after infarction.

Co-cultures of Treg and γδT cells

Single cell suspensions of peripheral (axillary, inguinal and submaxillary) lymph nodes of Foxp3-mRFP/IL17-eGFP/*cd69*$^{+/+}$ or Foxp3-mRFP/IL17-eGFP/*cd69*$^{-/-}$ reporter mice were stained with fluorochrome-conjugated antibodies. Treg cells ($CD3^+$Foxp3-$mRFP^+$) and γδT cells ($CD3^+$ $TCR\gamma\delta^+$ cells) were sorted using a BD FACSAria II cell sorter. Both cell populations were co-cultured at different ratios for 24h in the presence of plate-bound anti-CD3 (2 µg/ml) and soluble anti-CD28 (2 µg/ml) plus recombinant IL-2 (10 ng/ml) with or without ARL 67158 (250 µM, Tocris). Apoptosis of γδT cells was evaluated by flow cytometry using annexin V (BD Biosciences). For IL-17A-eGFP production assessment, cells were incubated 4 additional hours

in the presence of PMA (Sigma Aldrich), ionomycin (Sigma Aldrich) and GolgiPlug (BD PharMingen).

Extracellular ATP consumption assay

5 x 10^4 sorted Treg cells ($CD4^+$Foxp3-$mRFP^+$) from spleen were activated for three days in the presence of plate-bound anti-CD3 (3 µg/ml) and soluble anti-CD28 (2 µg/ml) plus recombinant IL-2 (10 ng/ml) in 96-well U-fond plates. After washing with PBS, cells were incubated for 40 minutes at 37 °C in complete RPMI medium (20% FBS, Gibco) in the presence of ATP (50 µM) and, when indicated, ARL 67158 (250 µM, Tocris). 50 µl of supernatants were collected at 20 and 40 minutes for extracellular ATP measurements. Cells were washed and used for FACS or qPCR analyses.

ATP concentration was quantified from the supernatants by firefly luciferase assay in 96-well luminescence reading plate (Costar). 50 µl of cell supernatant was diluted in 130 µl of Buffer A (150 mM KCl, 25 mM Tris HCl, 1 mM EDTA, 0,1 % BSA Fatty Acids free, 10 mM KH_2PO_4, pH 7.4). The reaction was started by adding 20 µl of luciferin/luciferase cocktail (0.5 M tris-acetate, 0.8 mM luciferin, 10 µg/ml luciferase, pH 7.4). Bioluminescent signal was read by Orion Microplate Luminometer, Simplicity 4.2 software. A regression curve for ATP concentration was calculated by a standard ATP curve measured in parallel in the same assay buffer.

RNA extraction and quantitative PCR

RNA was extracted from frozen human PBLs with MiRNeasy mini kit (Qiagen) as recommended by the manufacturer. Reverse transcription was performed from 200 ng of DNAse-treated RNA using the High Capacity cDNA RT kit (Applied Biosystems). Then, gene

expression was measured by real-time quantitative PCR using SYBR green PCR mix (*Applied Biosystems*) and mRNA specific primers (Thermo Fischer Scientific) for *Cd69* (Fw: 5' ATTGTCCAGGCCAATACACATT 3', Rv: 5' CCTCTCTACCTGCGTATCGTTTT 3'), *Foxp3* (Fw: 5' GAGAAGCTGAGTGCCATGCA 3', Rv: 5' GGAGCCCTTGTCGGATGAT 3'), *Gapdh* (Fw: 5' GAAGGTGAAGGTCGGAGTC 3', Rv: 5' GAAGATGGTGATGGGATTTC 3') and *Actb* (Fw: 5' CATCGAGCACGGCATCGTCA 3', Rv: 5' TAGCACAGCCTGGATAGCAAC 3'). Real-time qPCR analyses were performed with an ABI Prism 7900HT SDS 384-well thermal cycler (*Applied Biosystems*). Relative gene expression was determined using the $2^{-\Delta CT}$ method normalizing by both *Actb* and *Gapdh* housekeeping genes.

Statistics

For statistical analysis, the normality of the distributions was first evaluated using Shapiro-Wilk's test for mouse experiments and D'Agostino-Pearson's test for patient samples with higher n. If normal, unpaired Student's *t*-test was used for two-groups comparisons and one-way ANOVA with Tukey's *post hoc* test when more than two groups were compared. If distributions were non-normal, Mann-Whitney's U-test was used for the analysis of two groups and Kruskal-Wallis test with Dunn's *post hoc* test for multiple comparisons. In the kinetic experiments, two-way ANOVA with the Sidak's multiple comparison *post hoc* test was performed. Spearman´s correlation coefficient was used to analyze independence of continuous variables. Association between nominal variables was calculated by Chi-square (χ^2) test. Data analyses were performed with *GraphPad Prism 8.0* software. To assess the association of $CD69^+$ Treg cells with the development of HF, multivariate logistic regression analysis was performed adjusting for sex,

age, troponins (normalized values), CK and ejection fraction with R statistical software (version 3.6.2). In general, P-values below 0.05 were considered significant.

Study approval

Oral informed consent was obtained for patients requiring emergency coronary angiography and primary angioplasty and subsequently written informed consent was obtained immediately after the procedure. All participants included in the study were identified by number and provided authorization for the use of their medical records for research. The study was approved by the Research Ethics Committees from the hospitals *Universitario de la Princesa* and *Santa Creu i Sant Pau*.

All animal procedures were approved by the ethics committee of the Comunidad Autónoma de Madrid and conducted in accordance with the institutional guidelines that comply with European Institutes of Health directives (European Institutes of Health. 2010).

Author's contribution

PM and RBD contributed to study design, data analysis and manuscript production. RBD, LMA and AC executed and analyzed preclinical experiments. RBD, IRA, RSD, RJA and LMA contributed to patient blood sample processing and FACS. RBD analyzed the human data and coordinated the clinical database. HdlF, CR, MMGG, AD, MT, AV, JA, SCR, HB, MVO, FA and JMG provided clinical and/or scientific guidance and/or contributed to patients' samples collection and data analysis. PM contributed with study conception. All authors read and approved the final manuscript.

Acknowledgements

We thank Prof. Richard A. Flavell (Yale University, New Haven, CT) for kindly providing the *foxp3*-mRFP/*il-17 eGFP* double reporter mice. We thank the Veterinary Service of CNIC's Comparative Medicine Unit, Insourcing Solution Spain Charles River Laboratories, for performing the LAD-ligation surgeries in mice. We thank Ana Vanesa Alonso, Lorena Flores and Eva Sánchez de Rojas for their excellent technical work with the echocardiography acquisition and analysis in mice. We also thank all patients and volunteers for agreeing to participate in this study.

This study was supported by competitive grants from the *Ministerio de Ciencia e Innovación* (MCIN), through the Carlos III Institute of Health (ISCIII)-*Fondo de Investigación Sanitaria* (PI22/01759) to P.M.; RTI2018-094727-B-100 to J. M-G; *Comunidad de Madrid* grants S2017/BMD-3671-INFLAMUNE-CM to P.M. and FSM.*; Fundació La Marató* TV3 (20152330 31) to J.M-G and F.S-M.; *Ministerio de Ciencia e Innovación* (MCIN) RTI2018-099357-B-I00,

and CIBERFES (CB16/10/00282), Human Frontier Science Program (grant RGP0016/2018), and Leducq Transatlantic Networks (17CVD04) to JAE. AC is supported by Marie Skłodowska-Curie grant (agreement No. 713673). R.B-D. is supported by *Formación de Profesorado Universitario* (FPU16/02780) program from the Spanish Ministry of Education, Culture and Sports. The CNIC is supported by the ISCIII, the MCIN and the Pro CNIC Foundation, and is a Severo Ochoa Center of Excellence (SEV-2015-0505).

References

1. Swirski FK, and Nahrendorf M. Leukocyte behavior in atherosclerosis, myocardial infarction, and heart failure. *Science.* 2013;339(6116):161-166.

2. Swirski FK, and Nahrendorf M. Cardioimmunology: the immune system in cardiac homeostasis and disease. *Nat Rev Immunol.* 2018;18(12):733-744.

3. Hofmann U, et al. Activation of CD4+ T lymphocytes improves wound healing and survival after experimental myocardial infarction in mice. *Circulation.* 2012;125(13):1652-1663.

4. Hofmann U, and Frantz S. Role of T-cells in myocardial infarction. *Eur Heart J.* 2016;37(11):873-879.

5. Weiß E, et al. Myocardial-Treg Crosstalk: How to Tame a Wolf. *Front Immunol.* 2022;13(914033.

6. Rieckmann M, et al. Myocardial infarction triggers cardioprotective antigen-specific T helper cell responses. *J Clin Invest.* 2019;130(4922-4936.

7. Wang Y, et al. C-X-C Motif Chemokine Receptor 4 Blockade Promotes Tissue Repair After Myocardial Infarction by Enhancing Regulatory T Cell Mobilization and Immune-Regulatory Function. *Circulation.* 2019;139(15):1798-1812.

8. Seropian IM, et al. Galectin-1 controls cardiac inflammation and ventricular remodeling during acute myocardial infarction. *Am J Pathol.* 2013;182(1):29-40.

9. Weirather J, et al. Foxp3+ CD4+ T cells improve healing after myocardial infarction by modulating monocyte/macrophage differentiation. *Circ Res.* 2014;115(1):55-67.

10. Xia N, et al. Activated regulatory T-cells attenuate myocardial ischaemia/reperfusion injury through a CD39-dependent mechanism. *Clin Sci (Lond).* 2015;128(10):679-693.

11. George J, et al. Regulatory T cells and IL-10 levels are reduced in patients with vulnerable coronary plaques. *Atherosclerosis.* 2012;222(2):519-523.

12. Sardella G, et al. Frequency of naturally-occurring regulatory T cells is reduced in patients with ST-segment elevation myocardial infarction. *Thromb Res.* 2007;120(4):631-634.

13. Mao X, et al. IL-37 Plays a Beneficial Role in Patients with Acute Coronary Syndrome. *Mediators Inflamm.* 2019;2019(9515346.

14. Klingenberg R, et al. Clonal restriction and predominance of regulatory T cells in coronary thrombi of patients with acute coronary syndromes. *Eur Heart J.* 2015;36(17):1041-1048.

15. Cortes JR, et al. Maintenance of immune tolerance by Foxp3+ regulatory T cells requires CD69 expression. *J Autoimmun.* 2014;55(51-62.

16. Sanchez-Diaz R, et al. Thymus-Derived Regulatory T Cell Development Is Regulated by C-Type Lectin-Mediated BIC/MicroRNA 155 Expression. *Mol Cell Biol.* 2017;37(9).

17. Martin P, and Sanchez-Madrid F. CD69: an unexpected regulator of TH17 cell-driven inflammatory responses. *Sci Signal.* 2011;4(165):pe14.

18. Tsilingiri K, et al. Oxidized Low-Density Lipoprotein Receptor in Lymphocytes Prevents Atherosclerosis and Predicts Subclinical Disease. *Circulation.* 2019;139(2):243-255.

19. Cruz-Adalia A, et al. CD69 limits the severity of cardiomyopathy after autoimmune myocarditis. *Circulation.* 2010;122(14):1396-1404.

20. Barry SP, et al. Enhanced IL-17 signalling following myocardial ischaemia/reperfusion injury. *Int J Cardiol.* 2013;163(3):326-334.

21. Mora-Ruiz MD, et al. Role of interleukin-17 in acute myocardial infarction. *Mol Immunol.* 2019;107(71-78.

22. Yan X, et al. Temporal dynamics of cardiac immune cell accumulation following acute myocardial infarction. *J Mol Cell Cardiol.* 2013;62(24-35.

23. Yan X, et al. Deleterious effect of the IL-23/IL-17A axis and gammadeltaT cells on left ventricular remodeling after myocardial infarction. *J Am Heart Assoc.* 2012;1(5):e004408.

24. Chen XM, et al. Gene expression pattern of TCR repertoire and alteration expression of IL-17A gene of gammadelta T cells in patients with acute myocardial infarction. *J Transl Med.* 2018;16(1):189.

25. de la Fuente H, et al. The leukocyte activation receptor CD69 controls T cell differentiation through its interaction with galectin-1. *Mol Cell Biol.* 2014;34(13):2479-2487.

26. Lin CR, et al. Glycosylation-dependent interaction between CD69 and S100A8/S100A9 complex is required for regulatory T-cell differentiation. *Faseb j.* 2015;29(12):5006-5017.

27. Sreejit G, et al. Neutrophil-Derived S100A8/A9 Amplify Granulopoiesis After Myocardial Infarction. *Circulation.* 2020;141(13):1080-1094.

28. Hosono M, et al. Increased expression of T cell activation markers (CD25, CD26, CD40L and CD69) in atherectomy specimens of patients with unstable angina and acute myocardial infarction. *Atherosclerosis.* 2003;168(1):73-80.

29. Pasqui AL, et al. T cell activation and enhanced apoptosis in non-ST elevation myocardial infarction. *Clin Exp Med.* 2003;3(1):37-44.

30. Ibanez B, et al. 2017 ESC Guidelines for the management of acute myocardial infarction in patients presenting with ST-segment elevation: The Task Force for the management of acute myocardial infarction in patients presenting with ST-segment elevation of the European Society of Cardiology (ESC). *Eur Heart J.* 2018;39(2):119-177.

31. Shiow LR, et al. CD69 acts downstream of interferon-alpha/beta to inhibit S1P1 and lymphocyte egress from lymphoid organs. *Nature.* 2006;440(7083):540-544.

32. Bankovich AJ, et al. CD69 suppresses sphingosine 1-phosophate receptor-1 (S1P1) function through interaction with membrane helix 4. *J Biol Chem.* 2010;285(29):22328-22337.

33. Bohl S, et al. Refined approach for quantification of in vivo ischemia-reperfusion injury in the mouse heart. *Am J Physiol Heart Circ Physiol.* 2009;297(6):H2054-2058.

34. Stieger P, et al. Targeting of Extracellular RNA Reduces Edema Formation and Infarct Size and Improves Survival After Myocardial Infarction in Mice. *J Am Heart Assoc.* 2017;6(6).

35. Sano S, et al. Tet2-Mediated Clonal Hematopoiesis Accelerates Heart Failure Through a Mechanism Involving the IL-1β/NLRP3 Inflammasome. *J Am Coll Cardiol.* 2018;71(8):875-886.

36. Stevenson MD, et al. NADPH Oxidase 4 Regulates Inflammation in Ischemic Heart Failure: Role of Soluble Epoxide Hydrolase. *Antioxid Redox Signal.* 2019;31(1):39-58.

37. Bansal SS, et al. Dysfunctional and Proinflammatory Regulatory T-Lymphocytes Are Essential for Adverse Cardiac Remodeling in Ischemic Cardiomyopathy. *Circulation.* 2019;139(2):206-221.

38. Gonzalez-Amaro R, et al. Is CD69 an effective brake to control inflammatory diseases? *Trends Mol Med.* 2013;19(10):625-632.

39. Papotto PH, et al. IL-17(+) gammadelta T cells as kick-starters of inflammation. *Nat Immunol.* 2017;18(6):604-611.

40. Huber SA. T cells expressing the gamma delta T cell receptor induce apoptosis in cardiac myocytes. *Cardiovasc Res.* 2000;45(3):579-587.

41. Swirski FK, et al. Identification of splenic reservoir monocytes and their deployment to inflammatory sites. *Science.* 2009;325(5940):612-616.

42. Park SG, et al. T regulatory cells maintain intestinal homeostasis by suppressing gammadelta T cells. *Immunity.* 2010;33(5):791-803.

43. Kunzmann V, et al. Inhibition of phosphoantigen-mediated gammadelta T-cell proliferation by CD4+ CD25+ FoxP3+ regulatory T cells. *Immunology.* 2009;126(2):256-267.

44. Borsellino G, et al. Expression of ectonucleotidase CD39 by Foxp3+ Treg cells: hydrolysis of extracellular ATP and immune suppression. *Blood.* 2007;110(4):1225-1232.

45. Deaglio S, et al. Adenosine generation catalyzed by CD39 and CD73 expressed on regulatory T cells mediates immune suppression. *J Exp Med.* 2007;204(6):1257-1265.

46. Fabbiano S, et al. Immunosuppression-Independent Role of Regulatory T Cells against Hypertension-Driven Renal Dysfunctions. *Mol Cell Biol.* 2015;35(20):3528-3546.

47. Wang YM, et al. Regulatory T cells participate in CD39-mediated protection from renal injury. *Eur J Immunol.* 2012;42(9):2441-2451.

48. Mascanfroni ID, et al. Metabolic control of type 1 regulatory T cell differentiation by AHR and HIF1-α. *Nat Med.* 2015;21(6):638-646.

49. Cibrian D, et al. CD69 controls the uptake of L-tryptophan through LAT1-CD98 and AhR-dependent secretion of IL-22 in psoriasis. *Nat Immunol.* 2016;17(8):985-996.

50. Sharir R, et al. Experimental myocardial infarction induces altered regulatory T cell hemostasis, and adoptive transfer attenuates subsequent remodeling. *PLoS One.* 2014;9(12):e113653.

51. Pfeffer MA, et al. Development and prevention of congestive heart failure following myocardial infarction. *Circulation.* 1993;87(5 Suppl):Iv120-125.

52. Josefowicz SZ, et al. Regulatory T cells: mechanisms of differentiation and function. *Annu Rev Immunol.* 2012;30(531-564.

53. Shevach EM. Mechanisms of foxp3+ T regulatory cell-mediated suppression. *Immunity.* 2009;30(5):636-645.

54. Ohta A, and Sitkovsky M. Extracellular adenosine-mediated modulation of regulatory T cells. *Front Immunol.* 2014;5(304.

55. Cai M, et al. Transgenic over expression of ectonucleotide triphosphate diphosphohydrolase-1 protects against murine myocardial ischemic injury. *J Mol Cell Cardiol.* 2011;51(6):927-935.

56. Wheeler DG, et al. Transgenic swine: expression of human CD39 protects against myocardial injury. *J Mol Cell Cardiol.* 2012;52(5):958-961.

57. Smith SB, et al. Impact of cardiac-specific expression of CD39 on myocardial infarct size in mice. *Life Sci.* 2017;179(54-59.

58. Kohler D, et al. CD39/ectonucleoside triphosphate diphosphohydrolase 1 provides myocardial protection during cardiac ischemia/reperfusion injury. *Circulation.* 2007;116(16):1784-1794.

59. Lang RM, et al. Recommendations for cardiac chamber quantification by echocardiography in adults: an update from the American Society of Echocardiography and the European Association of Cardiovascular Imaging. *Eur Heart J Cardiovasc Imaging.* 2015;16(3):233-270.

Figure Legends

Figure 1. **Myocardial infarction patients present a strong peripheral CD69$^+$ Treg cell response.** (**A**) t-distributed stochastic neighbor embedding (t-SNE) plots of CD4$^+$ T cells from peripheral blood leukocytes from a representative healthy control and MI patient, considering the indicated markers measured by FACS. Color bars indicate the relative intensity of the markers. Dots represent individual cells. (**B**) Quantification of the percentages of CD4$^+$ and CD4$^+$CD25$^+$Foxp3$^+$ (Treg) cells in peripheral blood of healthy donors (n= 51) and MI patients (n= 215) at the time of hospital admission. (**C**) Percentages of CD69$^+$ Treg cells and CD69$^-$ Treg cells out of total peripheral blood leukocytes. (**D**) CD69 expression on Treg cells, quantified as percentage of CD69$^+$ cells after gating on Treg cells. Two groups of MI patients are differentiated according to the CD69 expression: patients with high levels of CD69 (High CD69), shown as black circles, and patients with low levels (Low CD69), as red circles. Representative histograms and percentages of CD69 expression on Treg cells are shown. In **B**-**D**, means ± SEM are indicated and data were analyzed by Mann-Whitney U-test. (**E**) Heat map shows the levels of the different cell populations analyzed by FACS and the cardiac damage markers in High CD69 and Low CD69 MI patients. Each column represents one patient. Data were normalized by subtracting the mean and dividing by the standard deviation. Color bar indicates the relative levels of each parameter with black indicating high expression and red, low expression. Differences between High and Low CD69 patients were analyzed by Mann-Whitney *U*-test, *$p< 0.05$, **$p< 0.01$, ****$p< 0.0001$. (**F**) t-SNE plot was made based on the percentages of the populations shown in **E** and analyzed by FACS. Dots represent individual MI patients. High CD69 and Low CD69 MI patients are show as black and red dots, respectively.

Figure 2. **CD69 deficiency worsens heart damage and decreases survival after myocardial infarction in mice.** (**A**) Survival curve of mice after LAD-ligation (n= 23-29 MI, n= 11-20 Sham). Data were pooled from five independent experiments and were analyzed by long-rank (Mantel-Cox) test. (**B**) Kinetics of the percentage of body weight loss after LAD-ligation (n= 9-17). Data represent means ± SEM and were analyzed by two-way ANOVA with Sidak's multiple comparisons test. * Differences between MI and Sham groups (gray for *Cd69*$^{+/+}$ mice, light red for *Cd69*$^{-/-}$ mice); $^{\&}$ differences between *Cd69*$^{+/+}$ and *Cd69*$^{-/-}$ MI mice. (**C**) Representative images of infarcted hearts collected after Evan's Blue intravenous injection at day 2 post-surgery. (**D**) Heart weight normalized versus body weight and tibia length at day 2 after LAD-ligation (n= 3-4 Sham mice and n= 5-6 MI mice). Data are representative of three independent experiments. Bars indicate means ± SEM and data were analyzed by one-way ANOVA with Tukey's post hoc test. (**E**) Representative images of heart slices showing area at risk (AAR, negative for Evans Blue) in upper panels and extent of necrosis (negative for triphenyltetrazoliumchloride, TTC staining) in lower panels. (**F**) Histological quantification of the percentage of the left-ventricular AAR and percentage of infarct size (n= 5-6). Data expressed as means ± SEM and analyzed by unpaired *t*-test. (**G**) Time course of the left-ventricular dysfunction according to the wall motions index (WMSI) measured by echocardiography (n= 6-16 MI, n= 4-8 Sham). Data were pooled from three independent experiments, represent means ± SEM and were analyzed by two-way ANOVA with Sidak's multiple comparisons test. *Differences between MI and Sham (grey for *Cd69*$^{+/+}$ mice, light red for *Cd69*$^{-/-}$ mice); $^{\&}$differences *Cd69*$^{+/+}$ and *Cd69*$^{-/-}$ MI mice; $^{+}$ differences between each day and day 0. $^{*/+/\&}p< 0.05$, $^{**/\&\&}p< 0.01$, $^{***/+++/\&\&\&}p< 0.001$, $^{****/++++/\&\&\&\&}p< 0.0001$.

Figure 3. **Treg and IL-17A responses in blood of mice after LAD-ligation**. (**A**) Fold Increase of the percentages of wild-type $CD69^+$ Treg cells, wild-type $CD69^-$ Treg cells and *Cd69*$^{-/-}$ Treg cells out of $CD4^+$ cells in peripheral blood one day after LAD-ligation/sham surgery, compared with the precentages at day 0 (dotted lines). Representative density plots of Treg cells at day 0 and day 1 post MI are shown on the right (n= 10-20). Histograms indicate means ± SEM and data were analyzed by one-way ANOVA with Tukey's post hoc test. (**B**). Kinetics of IL-$17A^+$ cells in peripheral blood after surgery, expressed as percentage of total cells. (**C**). Left, representative dot plots of IL-$17A^+$ cells, percentages of total cells are indicated inbox. Right, representative dot plots showing the main populations positive for IL-17A. (**D**). Kinetics of the percentages of γδT cells and IL-17^+ γδT cells in peripheral blood after LAD-ligation/sham surgery. Data in **B** and **D** are representative of four independent experiments and represent means ± SEM (n= 6-10). Data were analyzed by two-way ANOVA with Sidak's multiple comparisons test. * Differences between MI and Sham groups (in grey for *Cd69*$^{+/+}$ mice, in light red for *Cd69*$^{-/-}$ mice); $^{\&}$ differences between *Cd69*$^{+/+}$ and *Cd69*$^{-/-}$ MI mice; $^{+}$ differences between each day and day 0. $^{+/\&}$ $p< 0.05$, $^{**/++/\&\&}$ $p< 0.01$, $^{***/+++/\&\&\&}$ $p< 0.001$, $^{++++/\&\&\&\&}$ $p< 0.0001$.

Figure 4. **$CD69^+$ Treg and Il-17^+ γδT cells myocardial accumulation after LAD-ligation**. (**A**) Leukocyte cell number per milligram of heart tissue in the myocardium two days after infarction. (**B**) Quantification of the number of Treg ($CD4^+Foxp3^+$) cells and $CD4^+Foxp3^+CD69^+$ cells per mg of heart tissue and CD69 mean fluorescence expression on Treg cells in the heart. Representative density plots are shown after gating on $CD45^+CD11b^-CD4^+$ cells. (**C**) Representative density plots gated on $CD45^+CD11b^-CD3^+$ cells and numbers of γδT cells and Il-17^+ γδT cells per mg of tissue. (**D**) Quantification of total cell number per mg of $CD11b^+$

myeloid cells, $CD11b^{+}Gr1^{hi}$ cells and $CD11b^{+}F4/80^{lo}Ly6C^{hi}$ cells in the heart. Heart cell infiltrating populations were evaluated 2 days post infarction (n= 6-11 animals per group). Data are representative of four independent experiments. Bars indicate means ± SEM and data were analyzed by one-way ANOVA with Tukey's post hoc test. *P*-values of significant differences are shown.

Figure 5. **Expression of CD39 by $CD69^{+}$ Treg cells after myocardial infarction mediates the inhibition of γδT cells**. (**A**) Sorted wild-type γδT cells were co-cultured for 24h with *Cd69*$^{+/+}$ or *Cd69*$^{-/-}$ sorted Treg cells at the indicated γδT:Treg ratios. Apoptosis of γδT cells, represented as the fold increase of Annexin V^{+} γδT cells versus γδT cells alone (ratio 1:0) (n= 4-10). Representative zebra plot of the 1:0.5 ratio, gated on γδT cells, are shown. (**B**) Inhibition of IL-17A production by γδT cells, plotted as the fold change of IL-$17A^{+}$ γδT cells for each ratio versus the 1:0 ratio (n= 6-12). Representative zebra plots of the 1:0.5 ratio, gated on γδT cells, are shown. Data in **A** and **B** are a pool of four independent experiments. Means ± SEM. Two-way ANOVA with Sidak's multiple comparisons test. Significant *p*-values are shown (black for Treg *Cd69*$^{+/+}$ and red for Treg *Cd69*$^{-/-}$). (**C**) CD39 expression on Treg cells in PBL, mediastinal lymph nodes (Med-LN) and heart, measured by FACS, two days after MI (n= 4-5). Means ± SEM. One-way ANOVA with Tukey's *post hoc* test. (**D**) Extracellular ATP was measured in the supernatant of isolated Treg cells, in the presence or absence of ARL 67156 (ARL) at the indicated time points after ATP supplementation (n= 3-5). One representative out of four independent experiments. Means ± SEM. Mixed-effects two-way ANOVA with Sidak's multiple comparisons test. (**E**) IL-17A production by sorted γδT cells in the presence of Treg cells and/or ARL, fold change versus the percentage of IL-$17A^{+}$ γδT cells alone (n= 3-7). One representative

out of three independent experiments. Means ± SEM. Two-way ANOVA with Sidak's multiple comparisons test. (**F**) Quantification of *Ahr*, *Cyp1b1* and *Entpd1* mRNA levels in Treg cells by qPCR (n= 6-7). Data pooled from two independent experiments. Means ± SEM. Unpaired *t*-test.

Figure 6. **Adoptive transfer of CD69 sufficient Treg cells to *Cd69*$^{-/-}$ mice restores myocardial inflammation and survival after MI**. (**A**) Schematic workflow of the iTreg adoptive transfer after LAD-ligation. (**B**) Survival after LAD-ligation (n= 7-24). Black arrow depicts the time of iTreg cell inoculation (4-5h post-infarction). *Cd69*$^{-/-}$ mice without cell transfer were used as controls. *P*-value was calculated by long-rank (Mantel-Cox) test. (**C**) Heart-to-body weight ratio and total leukocyte number per mg of heart tissue 7 days after LAD-ligation (n= 5-6). (**D**) Representative density plots (gated on CD45^{+}CD11b^{-} cells) and numbers of γδT cells and IL-17^{+} γδT cells per mg of myocardial tissue. Data in **C**-**D** correspond to one representative out of three independent experiments, bars indicate means ± SEM and data were analyzed by one-way ANOVA with Tukey's post hoc test. (**E**) Survival after LAD-ligation (n= 12-13), *Cd69*$^{+/+}$ iTreg cell transfer and ARL or saline administration. Black arrow depicts the time of iTreg cell inoculation (4-5h post-infarction). *P*-value was calculated by long-rank (Mantel-Cox) test. (**F**) Total leukocyte number per mg of heart tissue 7 days after LAD-ligation (n= 9). (**G**) Numbers of γδT cells and IL-17^{+} γδT cells per mg of myocardial tissue (n= 9). Data in **F**-**G** are a pool of four independent experiments, bars indicate means ± SEM and data were analyzed by unpaired *t*-test.

Figure 7. High CD69 expression in patients early after MI is associated to decreased risk of heart failure development. (**A**) After 2.5 years of clinical follow-up, patients from the main study cohort were stratified depending on whether they have or have not developed heart failure

(HF). CD69 expression on Treg cells at the time of hospital admission by acute MI in patients developing HF (n= 7) or not developing HF (n =180). Data were analyzed by Mann-Whitney U-test. (**B**) Percentage of patients with low/high levels of surface CD69 expression on Treg cells, measured by FACS in the main study cohort. *P*-value was calculated by χ^2 test. (**C**) Frequency of patients with low/high levels of *CD69* mRNA, measured by qPCR in the main study cohort (the mean normalized Cd69 $2^{-\Delta Ct}$ values were used to discriminate low and high expressing patients). (**D**) Correlation of *FOXP3* and *CD69* mRNA expression in PBLs of the main study cohort. Spearman's correlation coefficient (r) and *P*-values are shown. (**E**) *CD69* mRNA levels measured by qPCR in total PBLs from the independent validation cohort of patients (n=75 No HF and n= 9 HF). Data were analyzed by Mann-Whitney U-test. (**F**) Frequency of patients with low/high levels of *CD69* mRNA, measured by qPCR in the validation cohort (the mean normalized *Cd69* $2^{-\Delta Ct}$ values were used to discriminate low and high expressing patients). *P*-value was calculated by χ^2 test. (**G**) Correlation of *FOXP3* and *CD69* mRNA expression in PBLs of the validation cohort. Spearman's correlation coefficient (r) and *P*-values are shown.

Tables

Table 1. Multivariable logistic regression model to discriminate patients with and without HF, adjusting for potential confounders. The General Linear Model (GLM) was used to assess the capability of variables to predict patients developing HF (n= 7) from those not developing heart failure (n= 180), in a model considering normalized troponin values, left ventricular (LV) ejection fraction, creatine kinase (CK), percentage of peripheral $CD69^+$ Treg cells, sex and age. CI, confidence interval.

	Odds ratio (95% CI)	***P*-value**
(Intercept)	0.000 (0.000-0.136)	0.0938
Troponins (Normalized)	0.992 (0.974-1.001)	0.2049
LV Ejection Fraction (%)	0.907 (0.759-1.044)	0.1888
CK (U/I)	1.001 (0.999-1.005)	0.4089
$CD69^+$ Treg cells (%)	**0.929 (0.838-0.980)**	**0.0409**
Sex	11.1 (0.404-4765.4)	0.2471
Age	**1.430 (1.128-2.482)**	**0.0444**

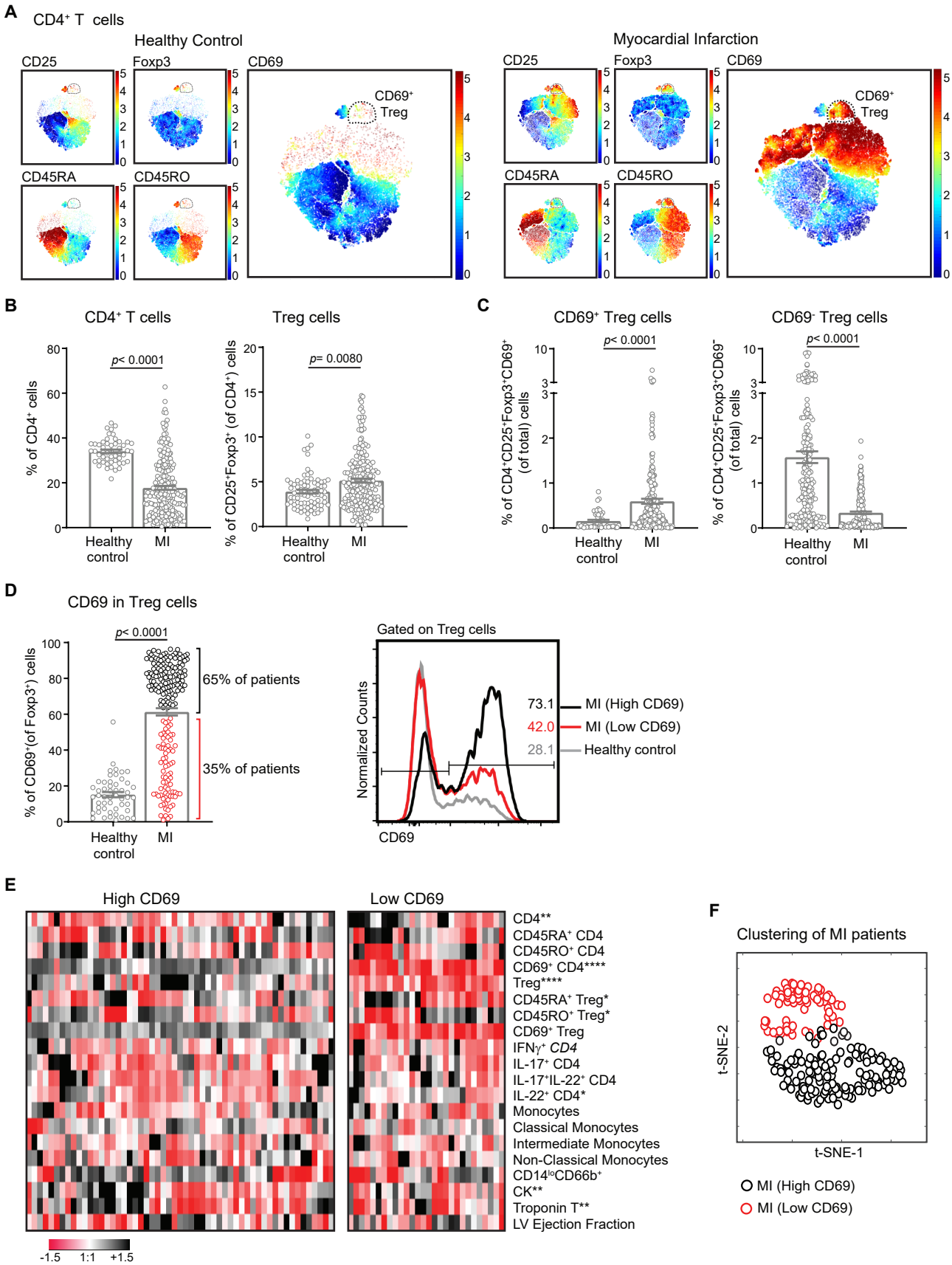
A
CD4+ T cells
Healthy Control
Myocardial Infarction
CD25
Foxp3
CD69
CD45RA
CD45RO
CD69+ Treg
B
CD4+ T cells
Treg cells
% of CD4+ cells
% of CD25+Foxp3+ (of CD4+) cells
p< 0.0001
p= 0.0080
Healthy control
MI
C
CD69+ Treg cells
CD69- Treg cells
% of CD4+CD25+Foxp3+CD69+ (of total) cells
% of CD4+CD25+Foxp3+CD69- (of total) cells
p< 0.0001
D
CD69 in Treg cells
% of CD69+(of Foxp3+) cells
65% of patients
35% of patients
Gated on Treg cells
Normalized Counts
CD69
73.1
42.0
28.1
MI (High CD69)
MI (Low CD69)
Healthy control
E
High CD69
Low CD69
CD4**
CD45RA+ CD4
CD45RO+ CD4
CD69+ CD4****
Treg****
CD45RA+ Treg*
CD45RO+ Treg*
CD69+ Treg
IFNγ+ CD4
IL-17+ CD4
IL-17+IL-22+ CD4
IL-22+ CD4*
Monocytes
Classical Monocytes
Intermediate Monocytes
Non-Classical Monocytes
CD14loCD66b+
CK**
Troponin T**
LV Ejection Fraction
-1.5
1:1
+1.5
F
Clustering of MI patients
t-SNE-2
t-SNE-1
MI (High CD69)
MI (Low CD69)

Figure 1

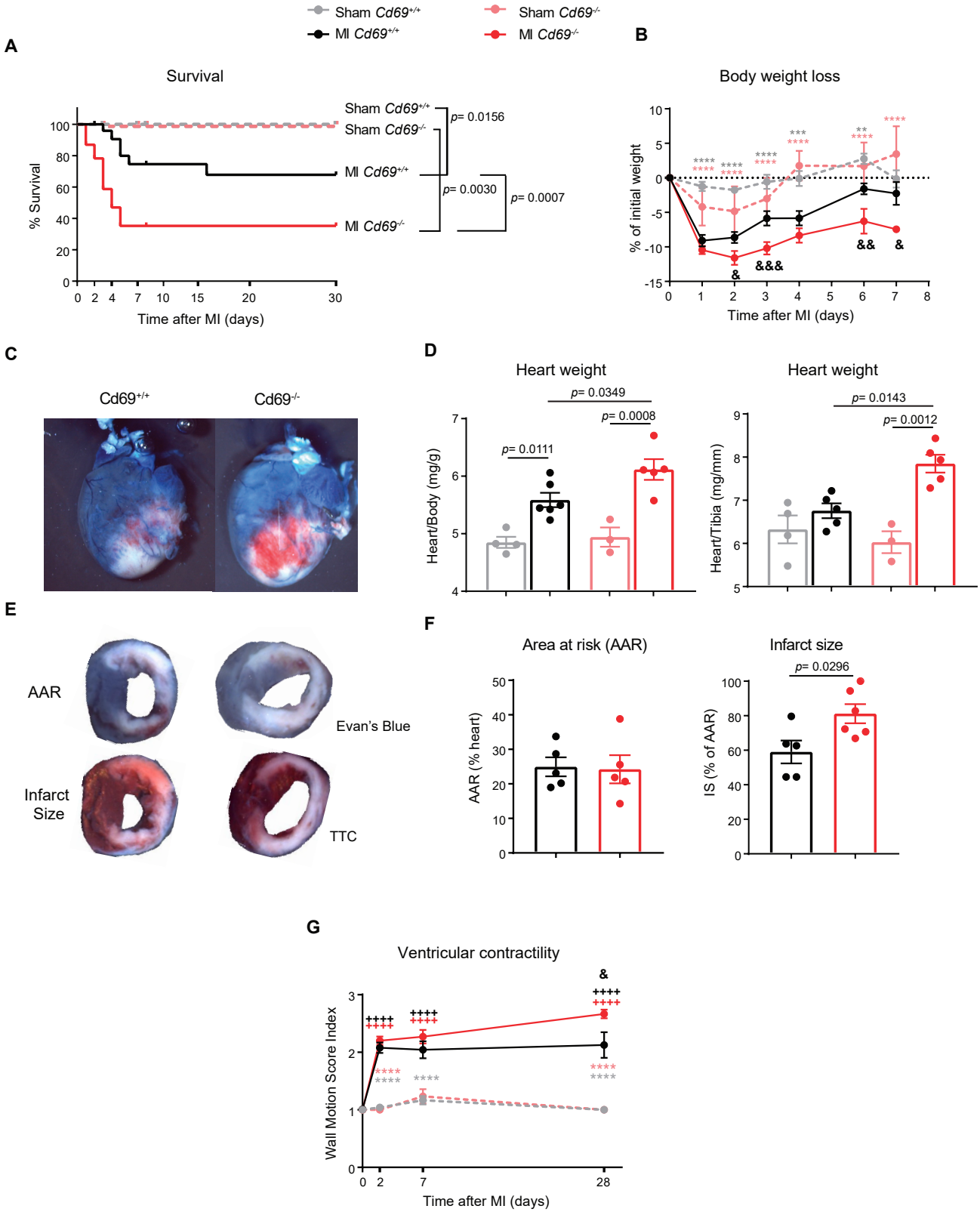
Sham Cd69+/+
MI Cd69+/+
Sham Cd69-/-
MI Cd69-/-
A
Survival
% Survival
Time after MI (days)
p= 0.0156
p= 0.0030
p= 0.0007
B
Body weight loss
% of initial weight
Time after MI (days)
C
Cd69+/+
Cd69-/-
D
Heart weight
Heart/Body (mg/g)
p= 0.0111
p= 0.0349
p= 0.0008
Heart weight
Heart/Tibia (mg/mm)
p= 0.0143
p= 0.0012
E
AAR
Evan's Blue
Infarct Size
TTC
F
Area at risk (AAR)
AAR (% heart)
Infarct size
IS (% of AAR)
p= 0.0296
G
Ventricular contractility
Wall Motion Score Index
Time after MI (days)

Figure 2

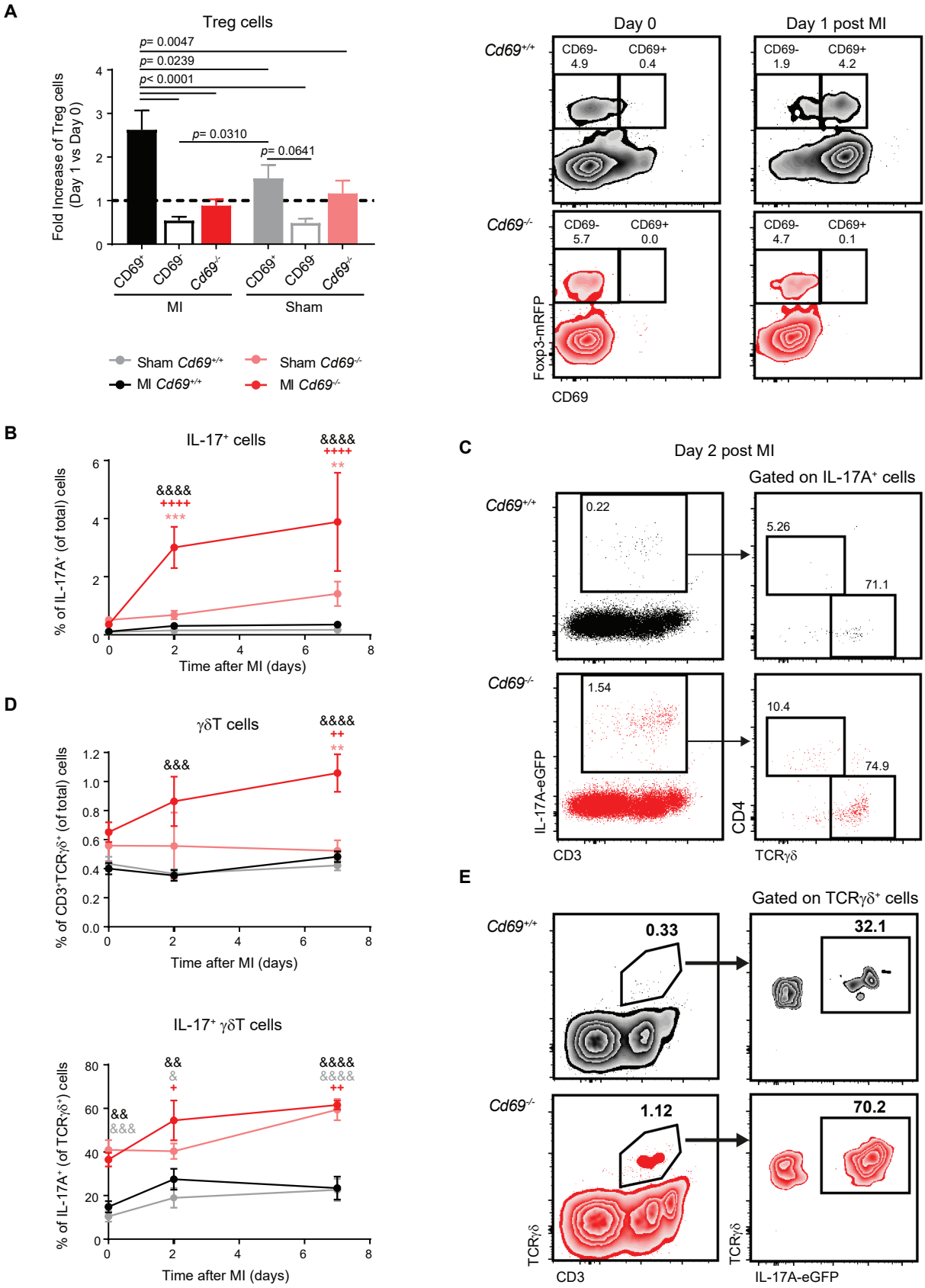
A
Treg cells
p= 0.0047
p= 0.0239
p< 0.0001
p= 0.0310
p= 0.0641
Fold Increase of Treg cells (Day 1 vs Day 0)
CD69+
CD69-
Cd69-/-
MI
Sham
Sham Cd69+/+
MI Cd69+/+
Sham Cd69-/-
MI Cd69-/-
Day 0
Day 1 post MI
Cd69+/+
CD69- 4.9
CD69+ 0.4
CD69- 1.9
CD69+ 4.2
Cd69-/-
CD69- 5.7
CD69+ 0.0
CD69- 4.7
CD69+ 0.1
Foxp3-mRFP
CD69
B
IL-17+ cells
% of IL-17A+ (of total) cells
Time after MI (days)
C
Day 2 post MI
Gated on IL-17A+ cells
Cd69+/+
0.22
5.26
71.1
Cd69-/-
1.54
10.4
74.9
IL-17A-eGFP
CD3
CD4
TCRγδ
D
γδT cells
% of CD3+TCRγδ+ (of total) cells
Time after MI (days)
IL-17+ γδT cells
% of IL-17A+ (of TCRγδ+) cells
Time after MI (days)
E
Gated on TCRγδ+ cells
Cd69+/+
0.33
32.1
Cd69-/-
1.12
70.2
TCRγδ
CD3
IL-17A-eGFP

Figure 3

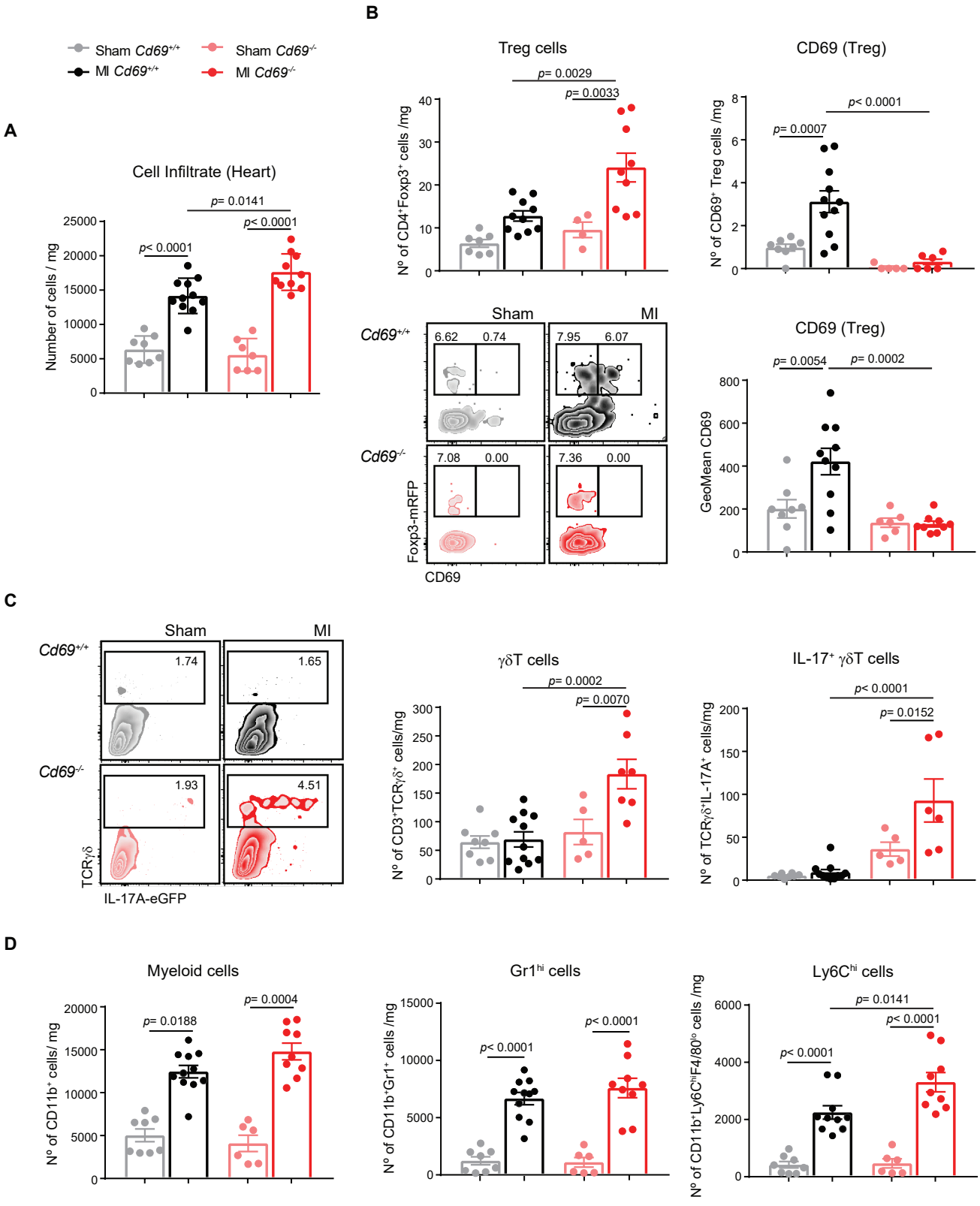
A
B
C
D
Sham Cd69+/+
MI Cd69+/+
Sham Cd69-/-
MI Cd69-/-
Cell Infiltrate (Heart)
Number of cells / mg
p= 0.0141
p< 0.0001
p< 0.0001
Treg cells
Nº of CD4+Foxp3+ cells /mg
p= 0.0029
p= 0.0033
CD69 (Treg)
Nº of CD69+ Treg cells /mg
p< 0.0001
p= 0.0007
Sham
MI
Cd69+/+
Cd69-/-
6.62
0.74
7.95
6.07
7.08
0.00
7.36
0.00
Foxp3-mRFP
CD69
CD69 (Treg)
GeoMean CD69
p= 0.0054
p= 0.0002
Sham
MI
Cd69+/+
Cd69-/-
1.74
1.65
1.93
4.51
TCRγδ
IL-17A-eGFP
γδT cells
Nº of CD3+TCRγδ+ cells/mg
p= 0.0002
p= 0.0070
IL-17+ γδT cells
Nº of TCRγδ+IL-17A+ cells/mg
p< 0.0001
p= 0.0152
Myeloid cells
Nº of CD11b+ cells/ mg
p= 0.0188
p= 0.0004
Gr1hi cells
Nº of CD11b+Gr1+ cells /mg
p< 0.0001
p< 0.0001
Ly6Chi cells
Nº of CD11b+Ly6ChiF4/80lo cells /mg
p< 0.0001
p= 0.0141
p< 0.0001

Figure 4

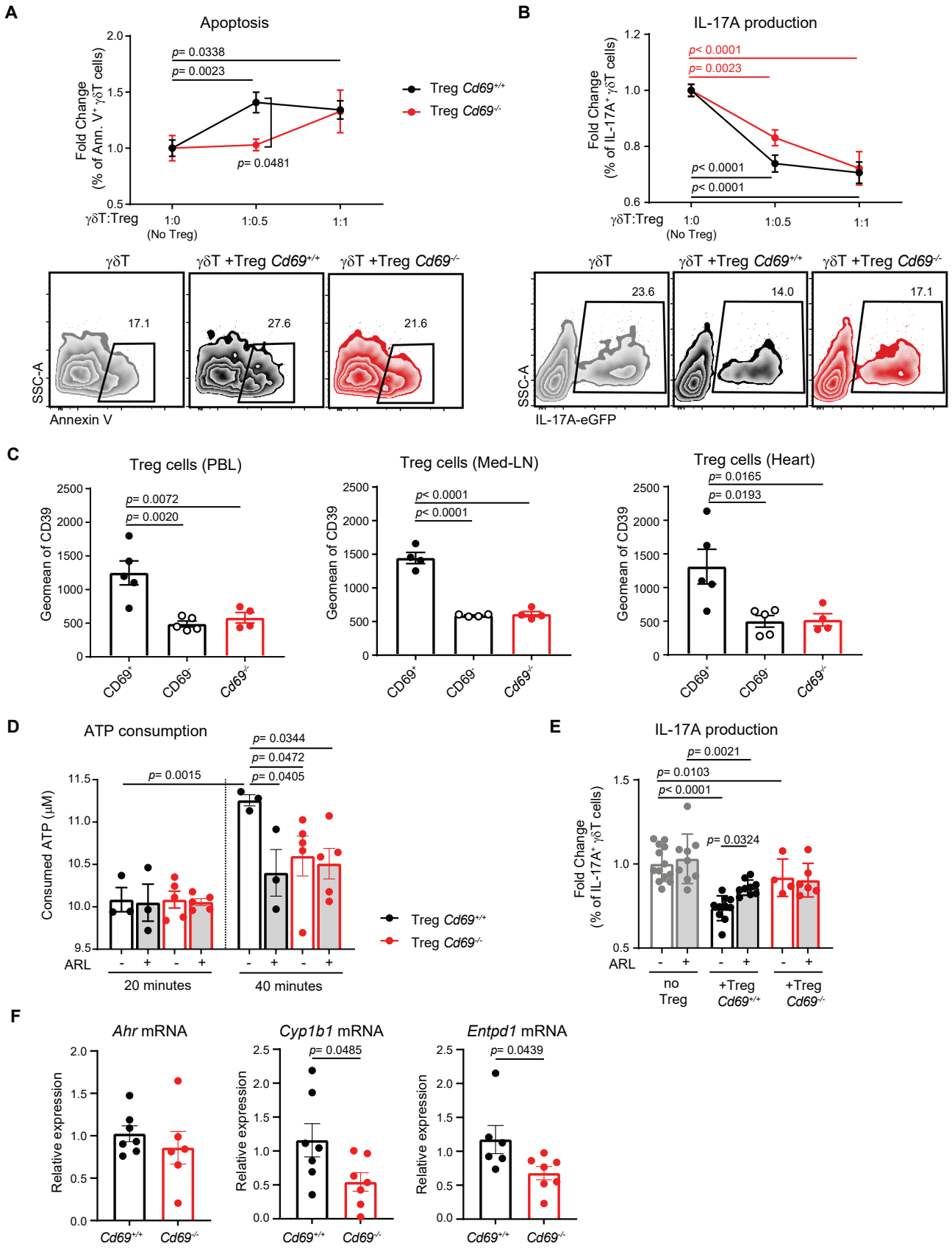
A
Apoptosis
Fold Change (% of Ann. V+ γδT cells)
p= 0.0338
p= 0.0023
p= 0.0481
Treg Cd69+/+
Treg Cd69-/-
γδT:Treg
1:0 (No Treg)
1:0.5
1:1
γδT
γδT +Treg Cd69+/+
γδT +Treg Cd69-/-
17.1
27.6
21.6
SSC-A
Annexin V
B
IL-17A production
Fold Change (% of IL-17A+ γδT cells)
p< 0.0001
p= 0.0023
p< 0.0001
p< 0.0001
23.6
14.0
17.1
IL-17A-eGFP
C
Treg cells (PBL)
Treg cells (Med-LN)
Treg cells (Heart)
Geomean of CD39
p= 0.0072
p= 0.0020
p< 0.0001
p< 0.0001
p= 0.0165
p= 0.0193
CD69+
CD69-
Cd69-/-
D
ATP consumption
Consumed ATP (μM)
p= 0.0015
p= 0.0344
p= 0.0472
p= 0.0405
ARL
20 minutes
40 minutes
E
IL-17A production
p= 0.0021
p= 0.0103
p< 0.0001
p= 0.0324
no Treg
+Treg Cd69+/+
+Treg Cd69-/-
F
Ahr mRNA
Cyp1b1 mRNA
Entpd1 mRNA
Relative expression
p= 0.0485
p= 0.0439

Figure 5

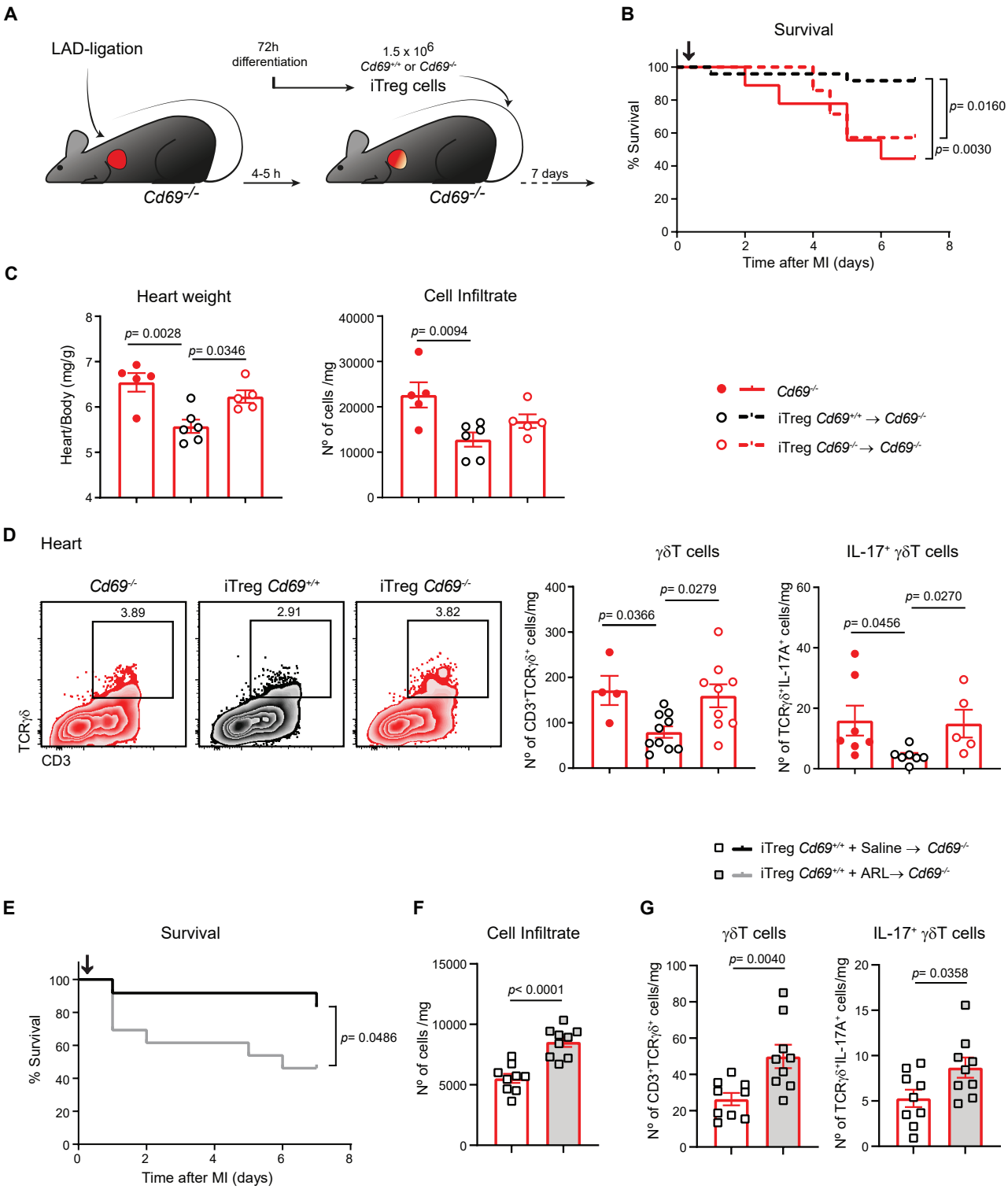
A
LAD-ligation
72h differentiation
1.5 x 10^6 Cd69+/+ or Cd69-/-
iTreg cells
4-5 h
7 days
Cd69-/-
Cd69-/-
B
Survival
% Survival
Time after MI (days)
p= 0.0160
p= 0.0030
C
Heart weight
Heart/Body (mg/g)
p= 0.0028
p= 0.0346
Cell Infiltrate
Nº of cells /mg
p= 0.0094
Cd69-/-
iTreg Cd69+/+ → Cd69-/-
iTreg Cd69-/- → Cd69-/-
D
Heart
Cd69-/-
iTreg Cd69+/+
iTreg Cd69-/-
3.89
2.91
3.82
TCRγδ
CD3
γδT cells
Nº of CD3+TCRγδ+ cells/mg
p= 0.0366
p= 0.0279
IL-17+ γδT cells
Nº of TCRγδ+IL-17A+ cells/mg
p= 0.0456
p= 0.0270
iTreg Cd69+/+ + Saline → Cd69-/-
iTreg Cd69+/+ + ARL→ Cd69-/-
E
Survival
% Survival
Time after MI (days)
p= 0.0486
F
Cell Infiltrate
Nº of cells /mg
p< 0.0001
G
γδT cells
Nº of CD3+TCRγδ+ cells/mg
p= 0.0040
IL-17+ γδT cells
Nº of TCRγδ+IL-17A+ cells/mg
p= 0.0358

Figure 6

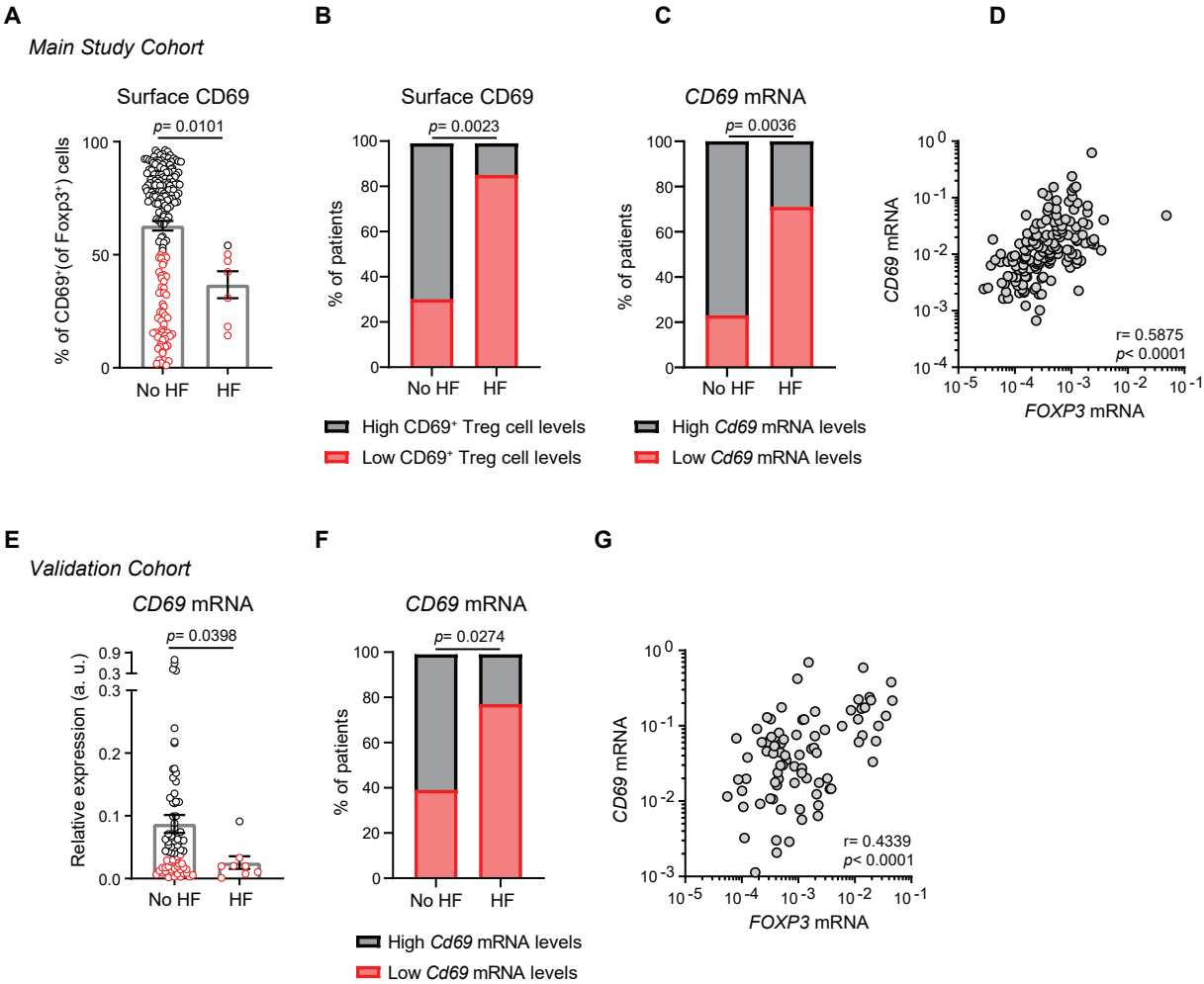
A
Main Study Cohort
Surface CD69
p= 0.0101
% of CD69+(of Foxp3+) cells
No HF
HF
B
Surface CD69
p= 0.0023
% of patients
High CD69+ Treg cell levels
Low CD69+ Treg cell levels
C
CD69 mRNA
p= 0.0036
% of patients
High Cd69 mRNA levels
Low Cd69 mRNA levels
D
CD69 mRNA
FOXP3 mRNA
r= 0.5875
p< 0.0001
E
Validation Cohort
CD69 mRNA
p= 0.0398
Relative expression (a. u.)
F
CD69 mRNA
p= 0.0274
% of patients
High Cd69 mRNA levels
Low Cd69 mRNA levels
G
CD69 mRNA
FOXP3 mRNA
r= 0.4339
p< 0.0001

Figure 7